

Detection and replication of epistasis influencing transcription in humans

Gibran Hemani^{1,2,*}, Konstantin Shakhbazov^{1,2}, Harm-Jan Westra³,
Tonu Esko^{4,5,6}, Anjali K Henders⁷, Allan F McRae^{1,2}, Jian Yang¹,
Greg Gibson⁸, Nicholas G Martin⁷, Andres Metspalu⁴, Lude
Franke³, Grant W Montgomery^{7,+}, Peter M Visscher^{1,2,+}, and
Joseph E Powell^{1,2,+}

¹Queensland Brain Institute, University of Queensland, Brisbane, QLD, Australia. ²University of Queensland Diamantina Institute, University of Queensland, Princess Alexandra Hospital, Brisbane, Queensland, Australia. ³Department of Genetics, University Medical Center Groningen, University of Groningen, Hanzeplein 1, Groningen, the Netherlands. ⁴Estonian Genome Center, University of Tartu, Tartu, 51010, Estonia. ⁵Medical and Population Genetics, Broad Institute, Cambridge, MA, 02142, US. ⁶Divisions of Endocrinology, Children's Hospital, Boston, MA, 02115, US. ⁷Queensland Institute of Medical Research, Brisbane, Queensland, Australia. ⁸School of Biology and Centre for Integrative Genomics, Georgia Institute of Technology, Atlanta, Georgia United States of America. ⁺These authors contributed equally. ^{*}Corresponding author: g.hemani@uq.edu.au

Abstract

Epistasis is the phenomenon whereby one polymorphism’s effect on a trait depends on other polymorphisms present in the genome. The extent to which epistasis influences complex traits¹ and contributes to their variation^{2,3} is a fundamental question in evolution and human genetics. Though often demonstrated in artificial gene manipulation studies in model organisms,^{4,5} and some examples have been reported in other species,⁶ few examples exist for epistasis amongst natural polymorphisms in human traits.^{7,8} Its absence from empirical findings may simply be due to low incidence in the genetic control of complex traits,^{2,3} but an alternative view is that it has previously been too technically challenging to detect due to statistical and computational issues.⁹ Here we show that, using advanced computation¹⁰ and a gene expression study design, many instances of epistasis are found between common single nucleotide polymorphisms (SNPs). In a cohort of 846 individuals with 7339 gene expression levels measured in peripheral blood, we found 501 significant pairwise interactions between common SNPs influencing the expression of 238 genes ($p < 2.91 \times 10^{-16}$). Replication of these interactions in two independent data sets^{11,12} showed both concordance of direction of epistatic effects ($p = 5.56 \times 10^{-31}$) and enrichment of interaction p -values, with 30 being significant at a conservative threshold of $p < 0.05/501$. Forty-four of the genetic interactions are located within 2Mb of regions of known physical chromosome interactions¹³ ($p = 1.8 \times 10^{-10}$). Epistatic networks of three SNPs or more influence the expression levels of 129 genes, whereby one *cis*-acting SNP is modulated by several *trans*-acting SNPs. For example MBNL1 is influenced by an additive effect at rs13069559 which itself is masked by *trans*-SNPs on 14 different chromosomes, with nearly identical genotype-phenotype (GP) maps for each *cis-trans* interaction. This study presents the first evidence for multiple instances of segregating common polymorphisms interacting to influence human traits.

Main text

In the genetic analysis of complex traits it is usual for SNP effects to be estimated using an additive model where they are assumed to contribute independently and cumulatively to the mean of a trait. This framework has been successful in identifying thousands of associations.¹⁴ But to date, though its contribution to phenotypic variance is frequently the subject of debate,¹⁻³ there is little empirical exploration of the role that epistasis plays in the architecture of complex traits in humans.^{7,8} Beyond the prism of human association studies there is evidence for epistasis, not only at the molecular scale from artificially induced mutations⁴ but also at the evolutionary scale in fitness adaptation¹⁵ and speciation.¹⁶

Methods are now available to overcome the computational problems involved in searching for epistasis, but its detection still remains problematic due to reduced statistical power. For example, increased dependence on linkage disequilibrium (LD) between causal SNPs and observed SNPs,^{17,18} increased model

complexity in fitting interaction terms,¹⁹ and more extreme significance thresholds to account for increased multiple testing⁹ all make it more difficult to detect epistasis in comparison to additive effects. Thus, with small genetic effect sizes, as is expected in most complex traits of interest,¹⁴ the power to detect epistasis diminishes rapidly. There are two simple ways to overcome this problem. One is by using extremely large sample sizes;²⁰ another is by analysing traits that are likely to have large effect sizes among common variants. Because our focus was to ascertain the extent to which instances of epistasis arises from natural genetic variation we designed a study around the latter approach and searched for epistatic genetic effects that influence gene expression levels. Transcription levels can be measured for thousands of genes and like most complex diseases, these expression traits are typically heritable.²¹ But unlike complex diseases, genetic associations with gene expression commonly have very large effect sizes that explain large proportions of the genetic variance,²² making them good candidates to search for epistasis, should it exist.

In our discovery dataset (Brisbane Systems Genetics Study, BSGS²³) of 846 individuals genotyped at 528,509 SNPs, we used a two stage approach to identify genetic interactions. First, we exhaustively test every pair of SNPs for pairwise effects against each of 7339 expression traits in peripheral blood (1.03×10^{15} statistical tests, family-wise error rate of 5% corresponding to a significance threshold of $p < 2.91 \times 10^{-16}$, Methods). Second, we filtered the SNP pairs from stage 1 on LD and genotype class counts, and tested the remaining pairwise effects for significant interaction terms and used a Bonferroni correction for multiple testing (estimated type 1 error rate $0.05 \leq \alpha \leq 0.14$, Methods, Supplementary Figure S1). Using this design we identified 501 putative genetic interactions influencing the expression levels of 238 genes (Supplementary Table S1). We used strict quality control measures to avoid statistical associations being driven by technical artifacts (Methods). However it remains possible that unexplained technical artifacts may have led to the significant discovery interactions. Of the 501 discovery interactions, 434 had available data and passed filtering (Methods) in two independent replication datasets, Fehrmann¹² and the Estonian Genomics Centre University of Tartu (EGCUT),¹¹ in which we saw convincing evidence for replication. We used the summary statistics from the replication datasets to perform a meta analysis to obtain an independent p -value for the putative interactions, and 30 were significant after applying a Bonferroni correction for multiple testing (5% significance threshold $p < 0.05/501$, Table 1). To quantify the similarity of GP maps between the independent datasets (Figure 1) we decomposed the genetic effects of each of the SNP pairs into orthogonal additive, dominance and epistatic effects ($A1$, $A2$, $D1$, $D2$, $A1 \times A2$, $A1 \times D2$, $D1 \times A2$, $D1 \times D2$) and tested for concordance of the sign of the most significant effect (Supplementary Table S3, Methods). Sign concordance between the discovery and both replication datasets was observed in 22 out of the 30 significantly replicated interactions (expected value = 7.5 under the null hypothesis of no interactions, $p = 3.76 \times 10^{-8}$).

In addition, using the meta analysis from the replication samples only, we observed that 316 of the remaining 404 discovery SNP pairs had replication

interaction p -values more extreme than the 2.5% confidence interval of the quantile-quantile plot against the null hypothesis of no interactions where p -values are assumed to be uniformly distributed ($p \ll 1.0 \times 10^{-16}$, Figure 2 and Supplementary Figure S2). Concordance of the direction of the effect of the largest variance component was also highly significant ($p = 5.71 \times 10^{-31}$, Supplementary Table S3). The congruence of the epistatic networks in discovery and replication datasets is shown in Figure 3, demonstrating that these complex genetic patterns are common even across independent datasets. A further replication was attempted using the Centre for Health Discovery and Wellbeing (CHDWB) dataset,²⁴ but only 20 of the SNP pairs passed filtering because the sample size was small ($n = 139$), and likely due to insufficient power we found no evidence for replication (Supplementary Figure S6). It should be noted that although it is a necessary step to establish the veracity of the interactions from the discovery set, replication of epistatic effects in independent samples is difficult in practice due to LD (Methods).

Though seldom the focus of association studies, SNPs with known main effects are often tested for $A \times A$ genetic interactions,⁹ but our analysis suggests this is unlikely to be the best strategy for its detection. The majority of our discovery interactions comprised of one SNP that was significantly associated with the gene expression level in the discovery dataset, and one SNP that had no previous association²² (439 out of 501, Methods). Only nine interactions were between SNPs that both had known main effects while 64 were between SNPs that had no known main effects. Additionally, we observed that the largest epistatic variance component for the 501 interactions was equally divided amongst $A \times A$, $A \times D$, $D \times A$ and $D \times D$ at the discovery stage ($p = 0.22$ for departure from expectation). This is not surprising because these patterns of epistasis used for statistical decomposition are simply convenient orthogonal parameterisations of a two locus model, and are not intended to model biological function.²⁵

Of the discovery interactions, 26 were *cis-cis* acting (within 1Mb of the transcription start site, mean distance between SNPs was 0.53Mb), 462 were *cis-trans*-acting, and 13 were *trans-trans*-acting. We observed a wide range of significant GP maps (Figure 1) but the most common pattern of epistasis that we detected involved a *trans*-SNP masking the effect of an additive *cis*-SNP. For example, MBNL1 (involved in RNA modification and regulation of splicing²⁶) has a *cis* effect at rs13069559 which in turn is controlled by 13 *trans*-SNPs and one *cis*-SNP that each exhibit a masking pattern, such that when the *trans*-SNP is homozygous for the masking allele the decreasing allele of the *cis*-SNP no longer has an effect (Supplementary Figure S10). Each of these interactions has evidence for replication in at least one dataset and six are significantly replicated at the Bonferroni level (Supplementary Figure S3). We see similar epistatic networks involving multiple (eight or more) *trans*-acting SNPs for other gene expression levels too, for example TMEM149 (Supplementary Figure S11), NAPRT1 (Supplementary Figure S12), TRAPPC5 (Supplementary Figure S13), and CAST (Supplementary Figure S14). We observed that from pedigree analysis these five gene expression phenotypes had non-additive variance component

estimates within the 95th percentile of the 17,994 gene expression phenotypes that were analysed previously²² (Supplementary Table S2, Methods).

In total the 501 interactions comprised 781 unique SNPs, which we analysed for functional enrichment (Methods). We tested the SNPs for cell-type specific overlap with transcriptionally active chromatin regions, tagged by histone-3-lysine-4,tri-methylation (H3K4me3) chromatin marks, in 34 cell types²⁷ (Supplementary Figure S5). There was significant enrichment for *cis*-acting SNPs in haematopoietic cell types only ($p < 1 \times 10^{-4}$ for the three tissues with the strongest enrichment after adjusting for multiple testing). However *trans*-acting SNPs did not show any tissue specific enrichment ($p > 0.1$ for all tissues). This difference between *cis* and *trans* SNPs suggests different roles in epistatic interactions where tissue specificity is provided by the *cis* SNPs. There is also enrichment for *cis*-SNPs to be localised in regions with regulatory genomic features as measured by chromatin states²⁸ (Supplementary Figure S4).

We also demonstrate physical organisation of interacting loci within the cell, suggesting a mechanism by which biological function can lead to epistatic genetic variance. It has been shown that different chromosomal regions spatially colocalise in the cell through chromatin interactions.¹³ We cross-referenced our epistatic SNPs with a map of chromosome interacting regions ($n = 96,139$) in K562 blood cell lines²⁹ (Methods) and found that 44 epistatic interactions mapped to within 5Mb ($p < 1.8 \times 10^{-10}$), (Supplementary Figure S15). Interaction of distant loci may occur through physical proximity in transcriptional factories that organise across different chromosome regions and can regulate transcription of related genes.³⁰

Quantifying the importance of epistasis in complex traits in humans remains an open question. Here we are able to identify 238 gene expression traits with at least one significant interaction given our experiment-wide threshold, where the minimum estimated variance explained by the epistatic effects of any interaction was 2.1% of phenotypic variance. Taking results from our previously published eQTL²³ we calculated that 1848 of the 7339 gene expression levels analysed were influenced by additive effects where the estimated additive variance of a locus was 2.1% or greater. Thus, we can infer that the number of instances of large additive effects is significantly greater than the number of instances of large epistatic effects.

In terms of their contribution to complex traits a more important metric might be the proportion of the variance that the epistatic loci explain.² Taking all additive effects detected in Powell *et al* (2012) that have additive variance explaining 2.1% or greater of phenotypic variance, we calculated that the proportion of total phenotypic variance of all 7339 gene expression levels explained by additive effects alone was 2.16%. By contrast, the estimated epistatic variance from the interacting SNPs detected in this study on average explain a total of 0.22% of phenotypic variance, approximately ten times lower than the estimated additive variance. There are several caveats to this comparison which we discuss in the Methods.

Overall, we have demonstrated that it is possible to identify and replicate epistasis in complex traits amongst common human variants, despite the rela-

tive contribution of pairwise epistasis to phenotypic variation being small. The bioinformatic analysis of the significant epistatic loci suggests that there are a large number of possible mechanisms that can lead to non-additive genetic variation. Further research into such epistatic effects may provide a useful framework for understanding molecular mechanisms and complex trait variation in greater detail. With computational techniques and data now widely available the search for epistasis in larger datasets for traits of broader interest is warranted.

Methods Summary

We searched for pairwise epistasis exhaustively in the BSGS discovery dataset,²³ which comprises 846 individuals who are genotyped at 528,509 autosomal SNPs. Each individual had gene expression levels measured in peripheral blood at 7,339 probes representing 6,158 RefSeq genes (significant expression in $\geq 90\%$ of individuals). SNP pairs were modelled for full genetic effects, including marginal additive and dominance at both SNPs plus four interaction terms. We used permutation analysis to calculate an experiment-wide significance threshold of $T_e = 2.91 \times 10^{-16}$ at the 5% family-wise error rate (FWER). All SNP pairs with LD $r^2 > 0.1$ and $D'^2 > 0.1$ were removed to minimise the possibility of haplotype effects. All SNP pairs were required to have at least five data points in all nine genotype classes. If multiple SNP pairs were present on the same chromosomes for a particular expression trait then only the sentinel SNP pair was retained. Finally, a nested test contrasting the full genetic model against the marginal additive and dominance model was performed for each remaining SNP pair. The 501 significant SNP pairs were carried forward for replication in two independent datasets that used the same expression assays for analysing transcription in peripheral blood Fehrmann,¹² $n = 1240$; EGCUT,¹¹ ($n = 891$). A meta analysis on the interaction p -values from each replication dataset was performed to provide an overall replication statistic for each putative interaction.

Acknowledgements

We are grateful to the volunteers for their generous participation in these studies. We thank Bill Hill, Chris Haley and Lars Ronnegard for helpful discussions and comments.

This work could not have been completed without access to high performance GPGPU compute clusters. We acknowledge iVEC for the use of advanced computing resources located at iVEC@UWA (www.ivec.org), and the Multimodal Australian ScienceS Imaging and Visualisation Environment (MASSIVE) (www.massive.org.au). We also thank Jake Carroll and Irek Porebski from the Queensland Brain Institute Information Technology Group for HPC support.

The University of Queensland group is supported by the Australian National Health and Medical Research Council (NHMRC) grants 389892, 496667, 613601, 1010374 and 1046880, the Australian Research Council (ARC) grant

(DE130100691), and by National Institutes of Health (NIH) grants GM057091 and GM099568.

The QIMR researchers acknowledge funding from the Australian National Health and Medical Research Council (grants 241944, 389875, 389891, 389892, 389938, 442915, 442981, 496739, 496688 and 552485), the and the National Institutes of Health (grants AA07535, AA10248, AA014041, AA13320, AA13321, AA13326 and DA12854). We thank Anthony Caracella and Lisa Bowdler for technical assistance with the micro-array hybridisations.

The CHDWB study funding support from the Georgia Institute of Technology Research Foundation. The funders had no role in study design, data collection and analysis, decision to publish, or preparation of the manuscript

The Fehrmann study was supported by grants from the Celiac Disease Consortium (an innovative cluster approved by the Netherlands Genomics Initiative and partly funded by the Dutch Government (grant BSIK03009), the Netherlands Organization for Scientific Research (NWO-VICI grant 918.66.620, NWO-VENI grant 916.10.135 to L.F.), the Dutch Digestive Disease Foundation (MLDS WO11-30), and a Horizon Breakthrough grant from the Netherlands Genomics Initiative (grant 92519031 to L.F.). This project was supported by the Prinses Beatrix Fonds, VSB fonds, H. Kersten and M. Kersten (Kersten Foundation), The Netherlands ALS Foundation, and J.R. van Dijk and the Adessium Foundation. The research leading to these results has received funding from the European Communitys Health Seventh Framework Programme (FP7/2007-2013) under grant agreement 259867.

The EGCUT study received targeted financing from Estonian Government SF0180142s08, Center of Excellence in Genomics (EXCEGEN) and University of Tartu (SP1GVARENG). We acknowledge EGCUT technical personnel, especially Mr V. Soo and S. Smit. Data analyzes were carried out in part in the High Performance Computing Center of University of Tartu.

Author contributions

G.H., J.E.P., P.M.V., and G.W.M. conceived and designed the study. G.H., J.E.P., K.S., H-J.W., and J.Y. performed the analysis. T.E. and A.M. provided the EGCUT data. A.K.H., A.F.M., G.W.M., N.G.M., and J.E.P. provided the BSGS data. H-J.W. and L.F. provided the Fehrmann data. G.H. and J.E.P. wrote the manuscript with the participation of all authors.

Author information

The authors declare no financial competing interests.

Tables

Table 1: Epistatic interactions significant at the Bonferroni level in two replication sets

	Gene (chr.)	SNP 1 (chr.)	SNP 2 (chr.)	BSGS ²	Fehrmann ³	EGCUT ³	Meta ⁴
1	ADK (10)	rs2395095 (10)	rs10824092 (10)	6.69 ¹	18.33 ¹	21.21 ¹	39.82 ¹
2	ATP13A1 (19)	rs4284750 (19)	rs873870 (19)	5.30	12.18	3.25	14.23
3	C21ORF57 (21)	rs9978658 (21)	rs11701361 (21)	9.42	6.08	16.36	21.67
4	CSTB (21)	rs9979356 (21)	rs3761385 (21)	11.99	25.20	16.72	42.27
5	CTSC (11)	rs7930237 (11)	rs556895 (11)	7.16	18.76	15.06	33.53
6	FN3KRP (17)	rs898095 (17)	rs9892064 (17)	16.16	28.24	29.39	59.95
7	GAA (17)	rs11150847 (17)	rs12602462 (17)	13.91	19.98	12.99	32.60
8	HNRPH1 (5)	rs6894268 (5)	rs4700810 (5)	15.38	8.55	3.01	10.37
9	LAX1 (1)	rs1891432 (1)	rs10900520 (1)	19.16	18.60	11.22	29.24
10	MBNL1 (3)	rs16864367 (3)	rs13079208 (3)	13.49	16.25	24.74	41.56
11	MBNL1 (3)	rs7710738 (5)	rs13069559 (3)	7.92	2.55	7.89	9.28
12	MBNL1 (3)	rs2030926 (6)	rs13069559 (3)	7.10	0.91	5.80	5.53
13	MBNL1 (3)	rs2614467 (14)	rs13069559 (3)	5.74	4.13	2.22	5.30
14	MBNL1 (3)	rs218671 (17)	rs13069559 (3)	7.63	0.62	5.82	5.23
15	MBNL1 (3)	rs11981513 (7)	rs13069559 (3)	7.71	0.43	5.36	4.58
16	MBP (18)	rs8092433 (18)	rs4890876 (18)	5.40	7.06	21.91	28.73
17	NAPRT1 (8)	rs2123758 (8)	rs3889129 (8)	8.45	15.12	16.08	30.77
18	NCL (2)	rs7563453 (2)	rs4973397 (2)	7.31	7.51	6.33	12.70
19	PRMT2 (21)	rs2839372 (21)	rs11701058 (21)	4.81	0.69	4.47	4.06
20	RPL13 (16)	rs352935 (16)	rs2965817 (16)	4.98	3.79	14.41	17.24
21	SNORD14A (11)	rs2634462 (11)	rs6486334 (11)	7.31	13.11	10.96	23.22
22	TMEM149 (19)	rs807491 (19)	rs7254601 (19)	12.16	81.55	45.78	145.78
23	TMEM149 (19)	rs8106959 (19)	rs6926382 (6)	5.80	3.06	8.80	10.72
24	TMEM149 (19)	rs8106959 (19)	rs914940 (1)	6.22	3.36	6.96	9.20
25	TMEM149 (19)	rs8106959 (19)	rs2351458 (4)	7.30	0.04	9.61	8.00
26	TMEM149 (19)	rs8106959 (19)	rs6718480 (2)	8.55	3.31	5.15	7.36
27	TMEM149 (19)	rs8106959 (19)	rs1843357 (8)	6.21	3.72	3.33	6.00
28	TMEM149 (19)	rs8106959 (19)	rs9509428 (13)	9.44	0.10	5.75	4.47
29	TRA2A (7)	rs7776572 (7)	rs11770192 (7)	8.23	3.19	1.89	4.09
30	VASP (19)	rs1264226 (19)	rs2276470 (19)	5.09	0.94	5.14	4.95

¹ $-\log_{10} p$ -values for 4 *d.f.* interaction tests

² Discovery dataset

³ Independent replication dataset

⁴ Meta analysis of interaction terms between replication datasets only

Figures

Figure 1: **Replication of GP maps in two independent populations**

The GP maps for each epistatic interaction that is significant at the Bonferroni level in both replication datasets are shown. Each GP map consists of nine tiles where each tile represents the expression level for that two-locus genotype class. Phenotypes are for gene transcript levels (dark coloured tiles = high expression, light coloured tiles = low expression). Columns of GP maps are for each independent dataset. Rows of GP maps are for each of 30 significantly replicated interactions at the Bonferroni level, corresponding to the rows in Table 1. There is a clear trend of the GP maps replicating across all three datasets.

Figure 2: **Q-Q plots of interaction p -values from replication datasets**

The top panel shows all 434 discovery SNPs that were tested for interactions. Observed p -values (y -axis, $-\log_{10}$ scale) are plotted against the expected p -values (x -axis, $-\log_{10}$ scale). The multiple testing correction threshold for significance following Bonferroni correction is denoted by a dotted line. The bottom panel shows the same data as the top panel but excluding the 30 interactions that were significant at the Bonferroni level in the replication datasets. The shaded grey area represents the 5% confidence interval for the expected distribution of p -values. Dark blue points represent p -values that exceed the confidence interval, light blue are within the confidence interval.

Figure 3: **Discovery and replication of epistatic networks**

All 434 putative genetic interactions (edges) with data common to discovery and replication sets is shown, where black nodes represent SNPs and red nodes represent traits (gene expression probes). Three hundred and forty-five interactions had p -values exceeding the 2.5% confidence interval following meta analysis of the replication data. The remaining 89 interactions that did not replicate are depicted in grey. It is evident that a large proportion of the complex networks identified in the discovery set also exist in independent populations. An interactive version of this graph can be found here: http://kn3in.github.io/detecting_epi/

References

- ¹ Carlborg, O. & Haley, C. S. Epistasis: too often neglected in complex trait studies? *Nature Reviews Genetics* **5**, 618–25 (2004).
- ² Hill, W. G., Goddard, M. E. & Visscher, P. M. Data and Theory Point to Mainly Additive Genetic Variance for Complex Traits. *PLoS Genetics* **4** (2008).
- ³ Crow, J. F. On epistasis: why it is unimportant in polygenic directional selection. *Philosophical transactions of the Royal Society of London. Series B, Biological sciences* **365**, 1241–4 (2010).
- ⁴ Costanzo, M. *et al.* The genetic landscape of a cell. *Science (New York, N.Y.)* **327**, 425–31 (2010).
- ⁵ Bloom, J. S., Ehrenreich, I. M., Loo, W. T., Lite, T.-L. V. o. & Kruglyak, L. Finding the sources of missing heritability in a yeast cross. *Nature* 1–6 (2013).
- ⁶ Carlborg, O., Jacobsson, L., Ahgren, P., Siegel, P. & Andersson, L. Epistasis and the release of genetic variation during long-term selection. *Nature Genetics* **38**, 418–420 (2006).
- ⁷ Strange, A. *et al.* A genome-wide association study identifies new psoriasis susceptibility loci and an interaction between HLA-C and ERAP1. *Nature Genetics* **42**, 985–90 (2010).
- ⁸ Evans, D. M. *et al.* Interaction between ERAP1 and HLA-B27 in ankylosing spondylitis implicates peptide handling in the mechanism for HLA-B27 in disease susceptibility. *Nature Genetics* **43** (2011).
- ⁹ Cordell, H. J. Detecting gene-gene interactions that underlie human diseases. *Nature Reviews Genetics* **10**, 392–404 (2009).
- ¹⁰ Hemani, G., Theocharidis, A., Wei, W. & Haley, C. EpiGPU: exhaustive pairwise epistasis scans parallelized on consumer level graphics cards. *Bioinformatics (Oxford, England)* **27**, 1462–5 (2011).
- ¹¹ Metspalu, A. The Estonian Genome Project. *Drug Development Research* **62**, 97–101 (2004).
- ¹² Fehrmann, R. S. N. *et al.* Trans-eQTLs reveal that independent genetic variants associated with a complex phenotype converge on intermediate genes, with a major role for the HLA. *PLoS genetics* **7**, e1002197 (2011).
- ¹³ Lieberman-Aiden, E. *et al.* Comprehensive mapping of long-range interactions reveals folding principles of the human genome. *Science (New York, N.Y.)* **326**, 289–93 (2009).

- ¹⁴ Visscher, P. M., Brown, M. a., McCarthy, M. I. & Yang, J. Five years of GWAS discovery. *American journal of human genetics* **90**, 7–24 (2012).
- ¹⁵ Weinreich, D. M., Delaney, N. F., Depristo, M. a. & Hartl, D. L. Darwinian evolution can follow only very few mutational paths to fitter proteins. *Science (New York, N.Y.)* **312**, 111–4 (2006).
- ¹⁶ Breen, M. S., Kemena, C., Vlasov, P. K., Notredame, C. & Kondrashov, F. a. Epistasis as the primary factor in molecular evolution. *Nature* **490**, 535–538 (2012).
- ¹⁷ Weir, B. S. Linkage disequilibrium and association mapping. *Annual review of genomics and human genetics* **9**, 129–42 (2008).
- ¹⁸ Hemani, G., Knott, S. & Haley, C. An Evolutionary Perspective on Epistasis and the Missing Heritability. *PLoS Genetics* **9**, e1003295 (2013).
- ¹⁹ Marchini, J., Donnelly, P. & Cardon, L. R. Genome-wide strategies for detecting multiple loci that influence complex diseases. *Nature Genetics* **37**, 413–417 (2005).
- ²⁰ Lango Allen, H. *et al.* Hundreds of variants clustered in genomic loci and biological pathways affect human height. *Nature* **467**, 832–8 (2010).
- ²¹ Schadt, E. *et al.* Genetics of gene expression surveyed in maize, mouse and man. *Nature* **422**, 297–302 (2003).
- ²² Powell, J. E. *et al.* Congruence of Additive and Non-Additive Effects on Gene Expression Estimated from Pedigree and SNP Data. *PLoS Genetics* **9**, e1003502 (2013).
- ²³ Powell, J. E. *et al.* The Brisbane Systems Genetics Study: genetical genomics meets complex trait genetics. *PloS one* **7**, e35430 (2012).
- ²⁴ Preininger, M. *et al.* Blood-informative transcripts define nine common axes of peripheral blood gene expression. *PLoS genetics* **9**, e1003362 (2013).
- ²⁵ Cockerham, C. C. An extension of the concept of partitioning hereditary variance for analysis of covariances among relatives when epistasis is present. *Genetics* **39**, 859–882 (1954).
- ²⁶ Ho, T. H. *et al.* Muscleblind proteins regulate alternative splicing. *The EMBO journal* **23**, 3103–12 (2004).
- ²⁷ Trynka, G. *et al.* Chromatin marks identify critical cell types for fine mapping complex trait variants. *Nature genetics* **45**, 124–30 (2013).
- ²⁸ Hoffman, M., Buske, O., Wang, J. & Weng, Z. Unsupervised pattern discovery in human chromatin structure through genomic segmentation. *Nature Methods* **9**, 473–476 (2012).

- ²⁹ Lan, X. *et al.* Integration of Hi-C and ChIP-seq data reveals distinct types of chromatin linkages. *Nucleic acids research* **40**, 7690–704 (2012).
- ³⁰ Rieder, D., Trajanoski, Z. & McNally, J. G. Transcription factories. *Frontiers in genetics* **3**, 221 (2012).

Supplementary Figures

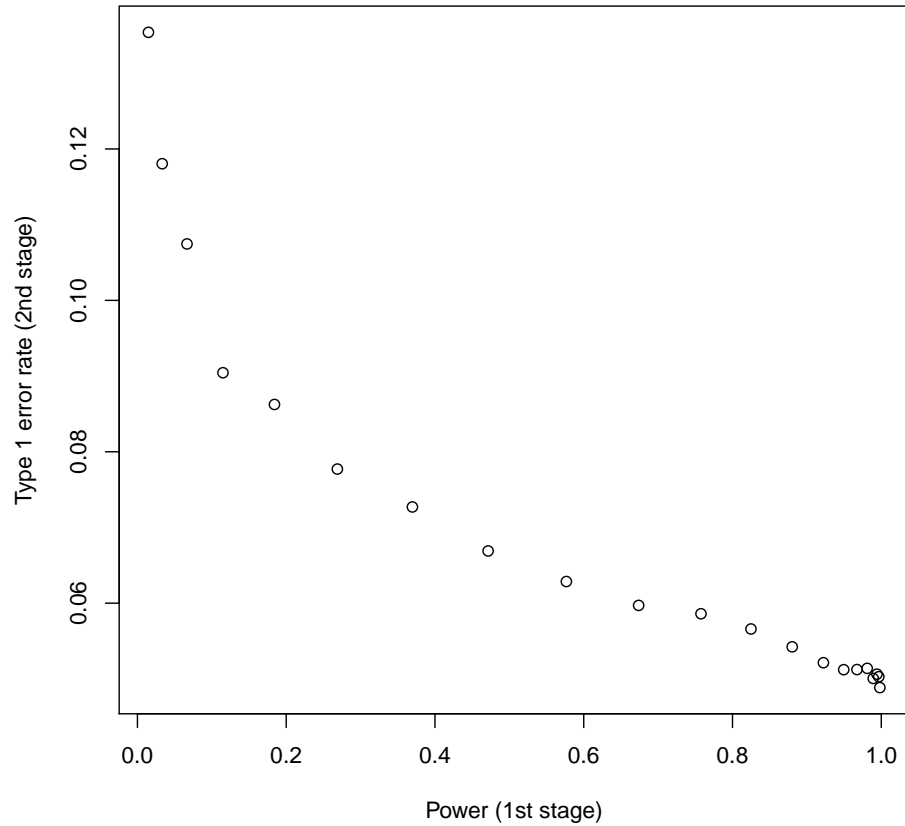


Figure S1: **Type 1 error rate of two stage design assuming a null model of one large additive effect and no epistasis** In stage 1 SNPs are tested for full genetic effects (8 d.f.) and those that surpass a threshold for multiple testing are then tested for significant interaction terms in stage 2. These interaction p -values are then adjusted (Bonferroni) for the total number of tests that passed stage 1. The type 1 error rate of this two stage design is dependent on the power, which is not known empirically.

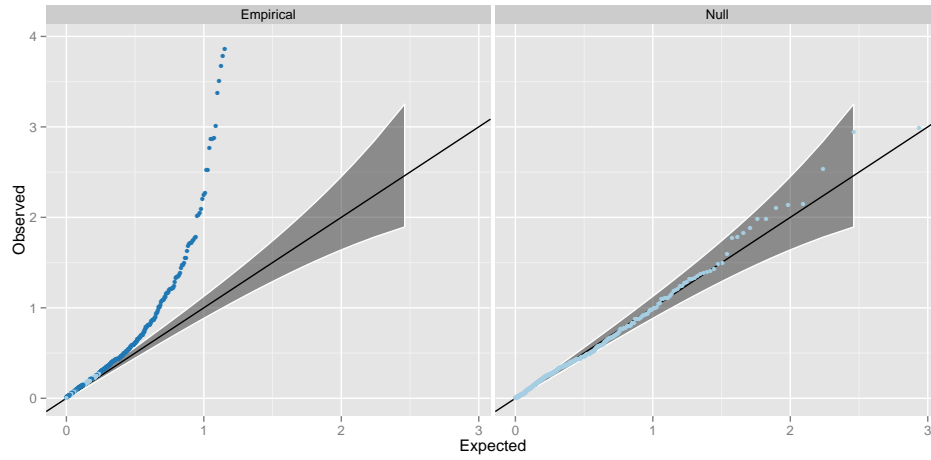


Figure S2: **Q-Q plots of interaction p -values from replication datasets, excluding the 30 points significant at the Bonferroni level** The right panel (Null) shows the interaction p -values from a meta analysis across two independent datasets on 434 SNP pairs where one SNP has a marginal effect. The left panel (Empirical) shows the interaction p -values from the 404 putative interactions that were not significant at the Bonferroni correction threshold. Dark blue points represent p -values that surpass the 2.5% FDR level, as in Figure 2.

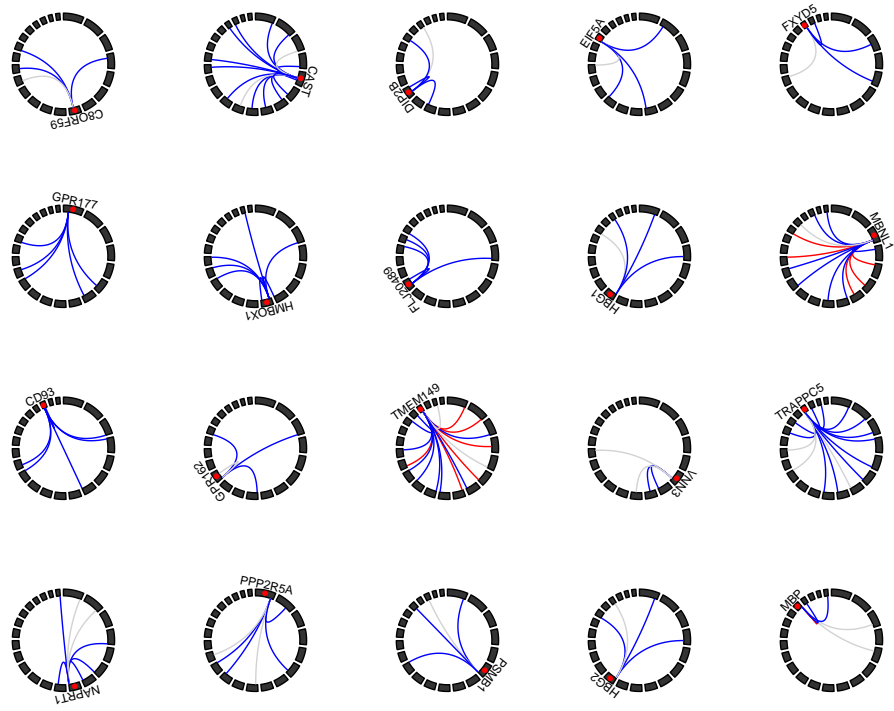


Figure S3: **Gene expression traits with four or more genetic interactions** Circle plots represent the genomic positions for SNPs (linking lines) and expression probes (red points). Chromosomes are represented by black blocks and ordered from 1 to 22 clockwise, starting from the top. Grey lines represent no evidence for replication, blue lines denote interactions that are outside the 97.5% confidence interval or the Q-Q plot (Figure 2), and red lines denote replication at the Bonferroni correction level. Most interactions are characterised as being *cis-trans* to the expression probe.

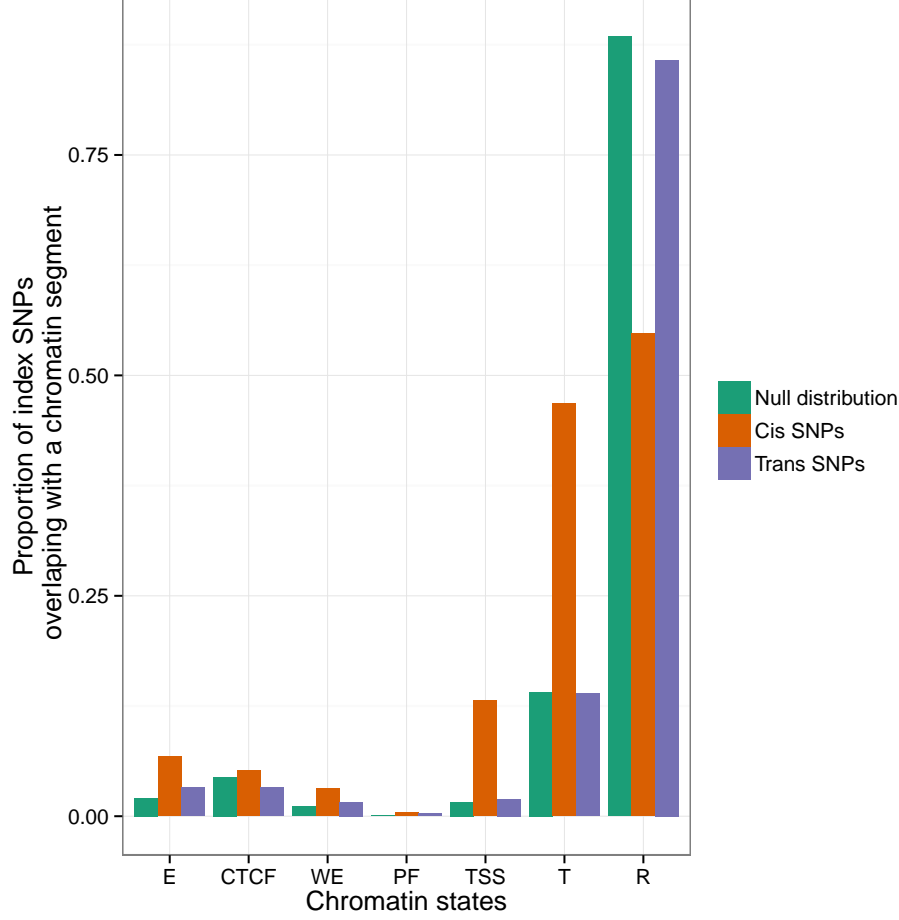


Figure S4: Location of SNPs relative to genomic features We used chromatin segmentation²⁸ as a method for labelling genomic features. All SNPs within 1Mb and $r^2 > 0.8$ of each *cis*- and *trans*-SNP were taken to find which genomic features (x -axis) were covered by the SNPs that compose the 501 significant interactions. Green bars represent the proportion (y -axis) of the 528,509 SNPs used in the analysis that fall within the range of the different genomic features. There is enrichment for *cis*-acting SNPs (red bars) in promotor regions, but *trans*-acting SNPs (blue bars) are not enriched for genomic features. The labels on the x -axis are as follows: E = Predicted enhancer, CTCF = CTCF enriched element, WE = Predicted weak enhancer or open chromatin cis regulatory element, PF = Predicted promoter flanking region, TSS = Predicted promoter region including transcriptional start site, T = Predicted transcribed region, R = Predicted Repressed or Low Activity region

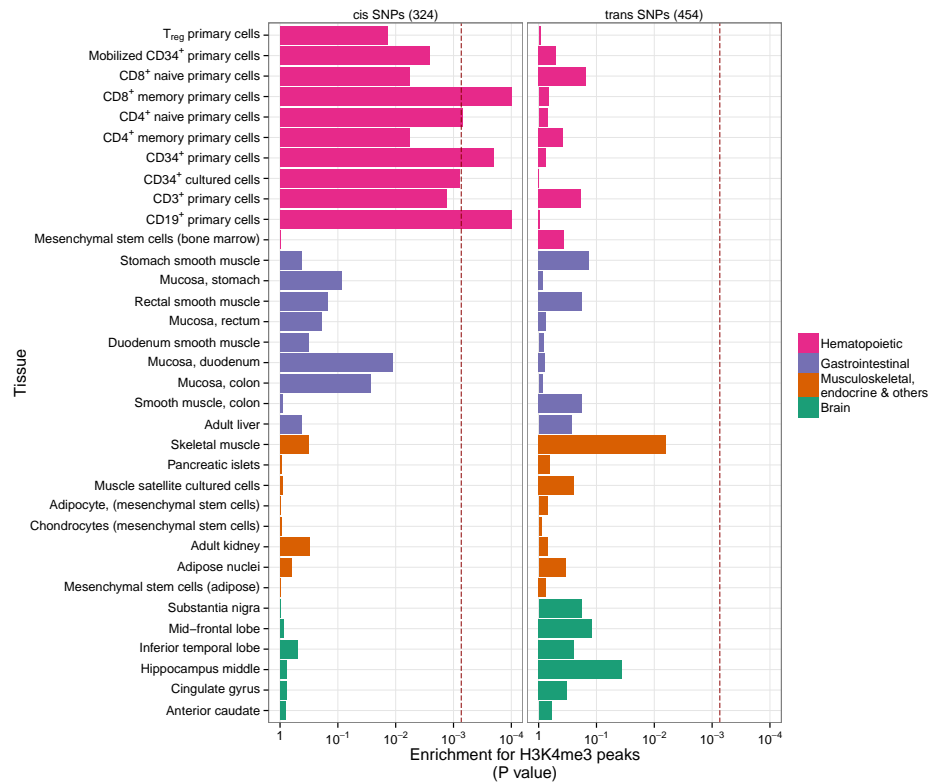


Figure S5: Tissue specific enrichment of SNPs in transcriptionally active regions The locations of transcriptional activity can be predicted by chromatin marks, assayed by H3K4me3.²⁷ Enrichment p -values are calculated using permutation analysis for 34 different cell types (y -axis) in four tissue types (Rows of boxes). The dotted red line denotes significance (Bonferroni correction for 34 cell types, x -axis). There is enrichment for *cis*-acting SNPs in Haematopoietic tissue types only. *Trans*-acting SNPs have no tissue specificity.

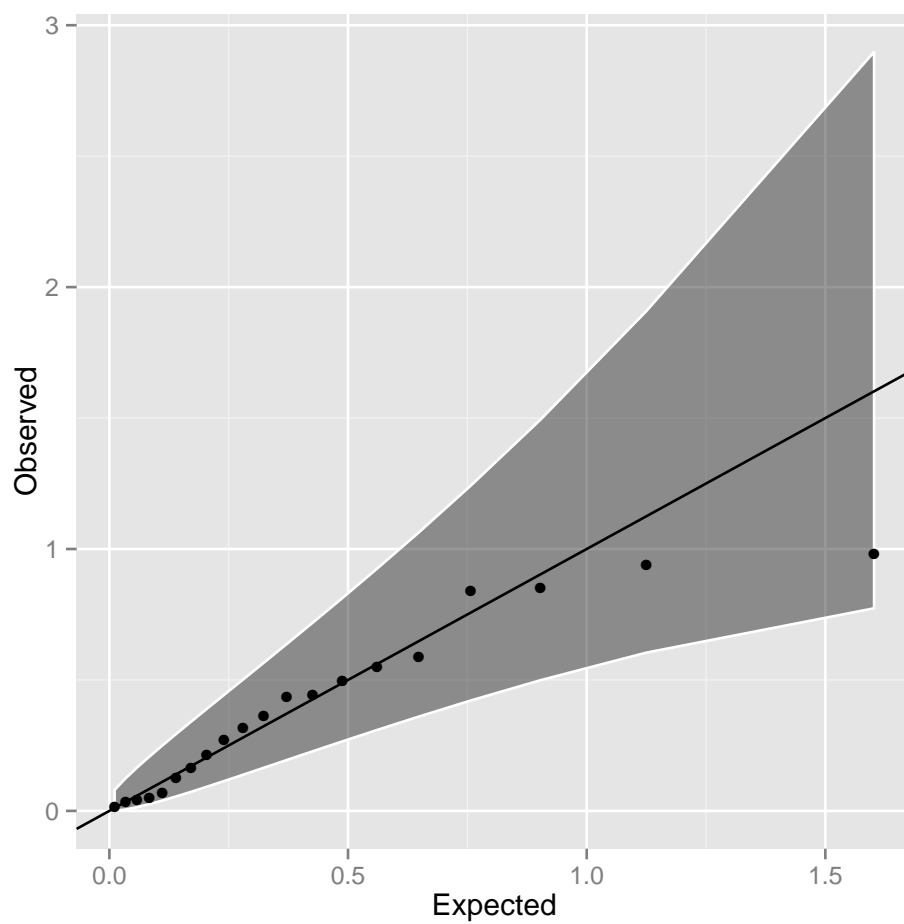


Figure S6: **Q-Q plot of interaction p -values in the CDHWB dataset**
 Twenty of the 501 discovery SNP pairs passed filtering in the CDHWB dataset (mainly due to small sample size). There is no evidence for enrichment of interaction terms, most likely due to insufficient power given the limited sample size.

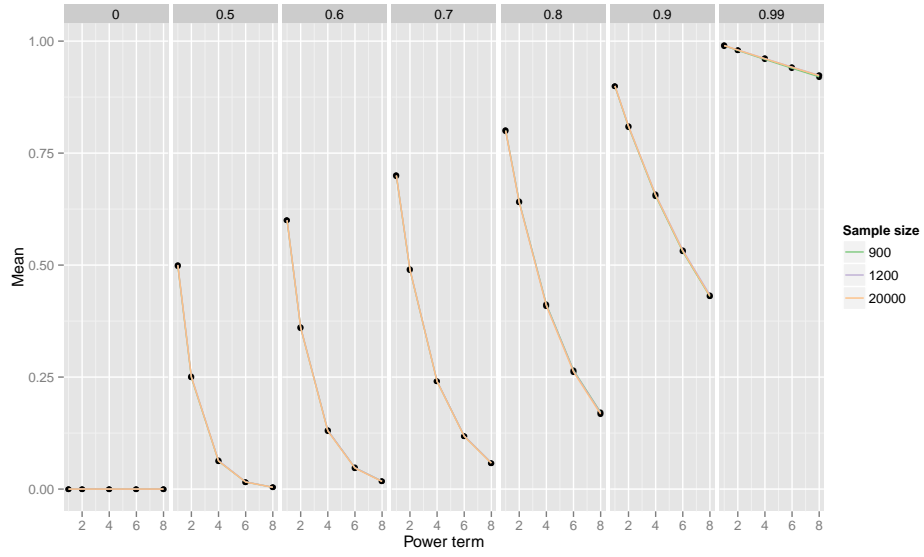


Figure S7: **Sampling mean for different power terms of population r values** Power of detection and replication of epistatic interactions depends not on r^2 between causal variants and observed SNPs, but on r^4, r^6, r^8 . For a given population value of LD r (columns of plots), plotted is the sample mean (y -axis) of \hat{r} , \hat{r}^2 (additive), \hat{r}^4 (dominance, $A \times A$), \hat{r}^6 ($A \times D$), \hat{r}^8 ($D \times D$) (x -axis) for different sample sizes (coloured lines). As true r reduces the statistical power to detect epistatic variants drops dramatically under the assumption that statistical power is proportional to higher moments of r .

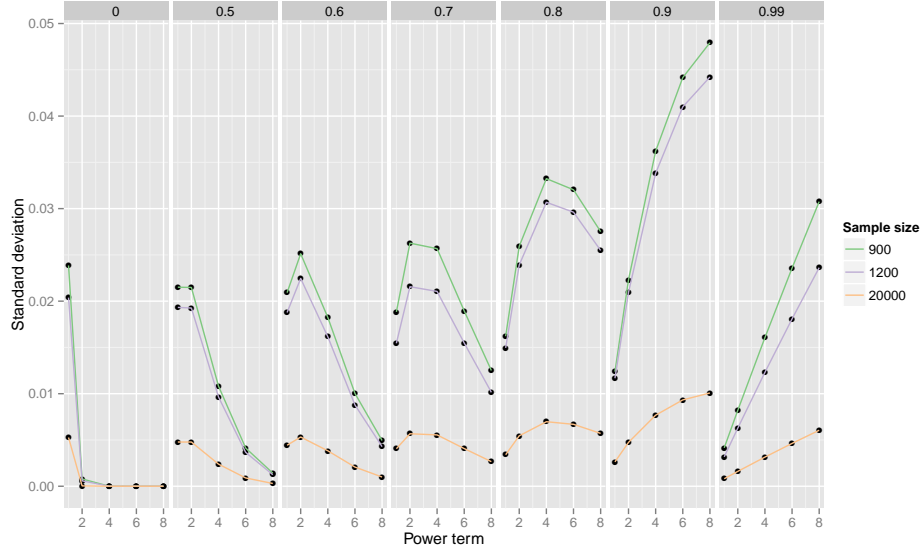


Figure S8: Sampling standard deviation for different power terms of population r values Power of detection and replication of epistatic interactions depends not on r^2 between causal variants and observed SNPs, but on r^4, r^6, r^8 . For a given a population value of LD r (columns of plots), plotted is the sampling standard deviation (y -axis) of \hat{r} , \hat{r}^2 (additive), \hat{r}^4 (dominance, $A \times A$), \hat{r}^6 ($A \times D$), \hat{r}^8 ($D \times D$) (x -axis) for different sample sizes (coloured lines). As the power term of r increases the sampling variance also increases. Supposing that there is sufficiently high r^x in the discovery sample for detection of epistasis, the replication sample is less likely to have similarly high r^x as x increases, leading to an expectation of reduced replication rates.

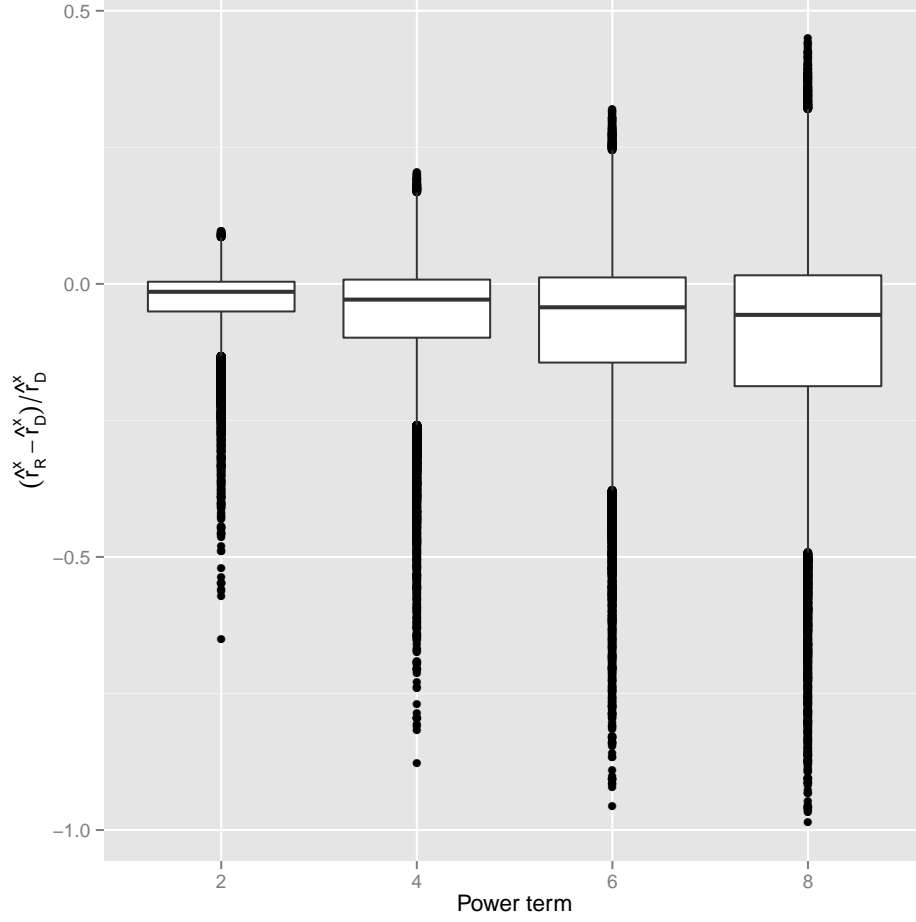


Figure S9: **Reduction in LD as estimated in replication data after ascertaining for high LD in discovery data** 100,000 “unobserved” causal variants (CVs) were tested for LD against a panel of 528,509 “observed” discovery markers (DMs). DM/CV pairs with LD $r^2 > 0.9$ were then tested in an independent sample. Simulation results of the proportional decrease between discovery and replication datasets in LD (y -axis) of $\hat{r}^2, \hat{r}^4, \hat{r}^6, \hat{r}^8$ (x -axis) are shown, where \hat{r}_D^x and \hat{r}_R^x are the sample LD measurements in the discovery and replication datasets, respectively. The average proportional decrease in the replication \hat{r}_R^x was 2.8%, 5.3%, 7.4% and 9.2% for $x = 2, 4, 6$ and 8, respectively.

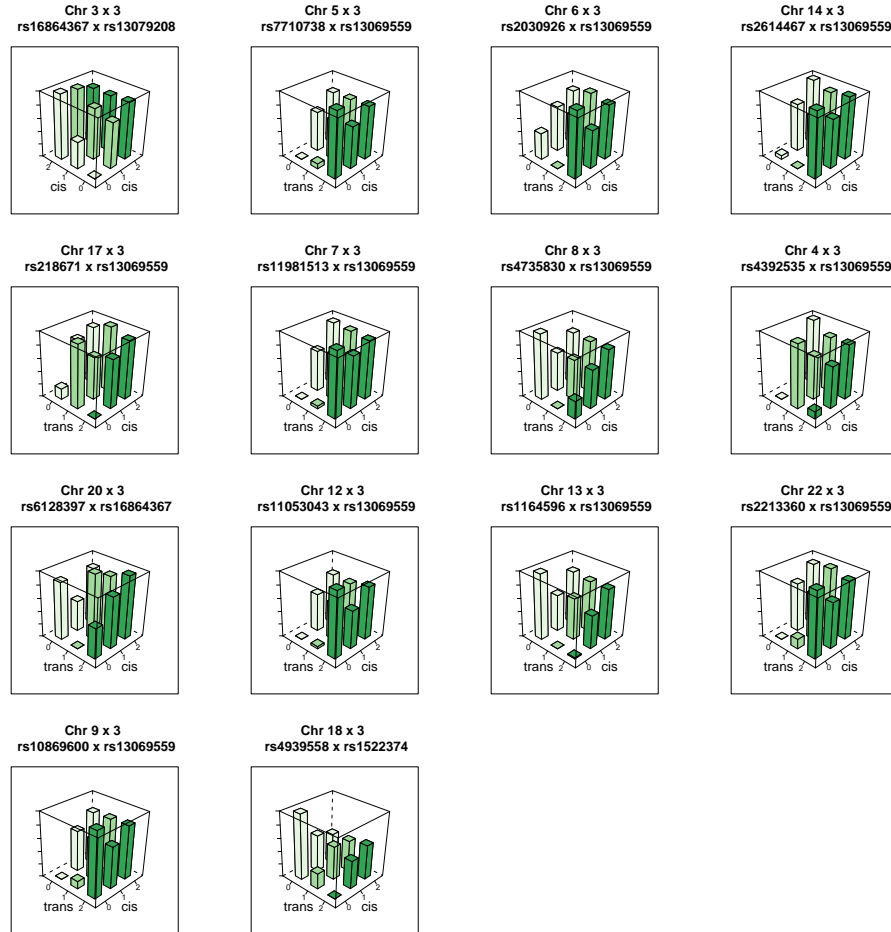


Figure S10: **Genotype-phenotype maps for 14 interactions influencing the expression of MBNL1** Each bar represents the mean phenotypic value for individuals in that genotype class. The rs13069559 SNP typically has a *cis*-additive decreasing effect on the expression of MBNL1, but in many of these interactions the *cis* effect is masked when the *trans* SNP is homozygous for the masking allele.

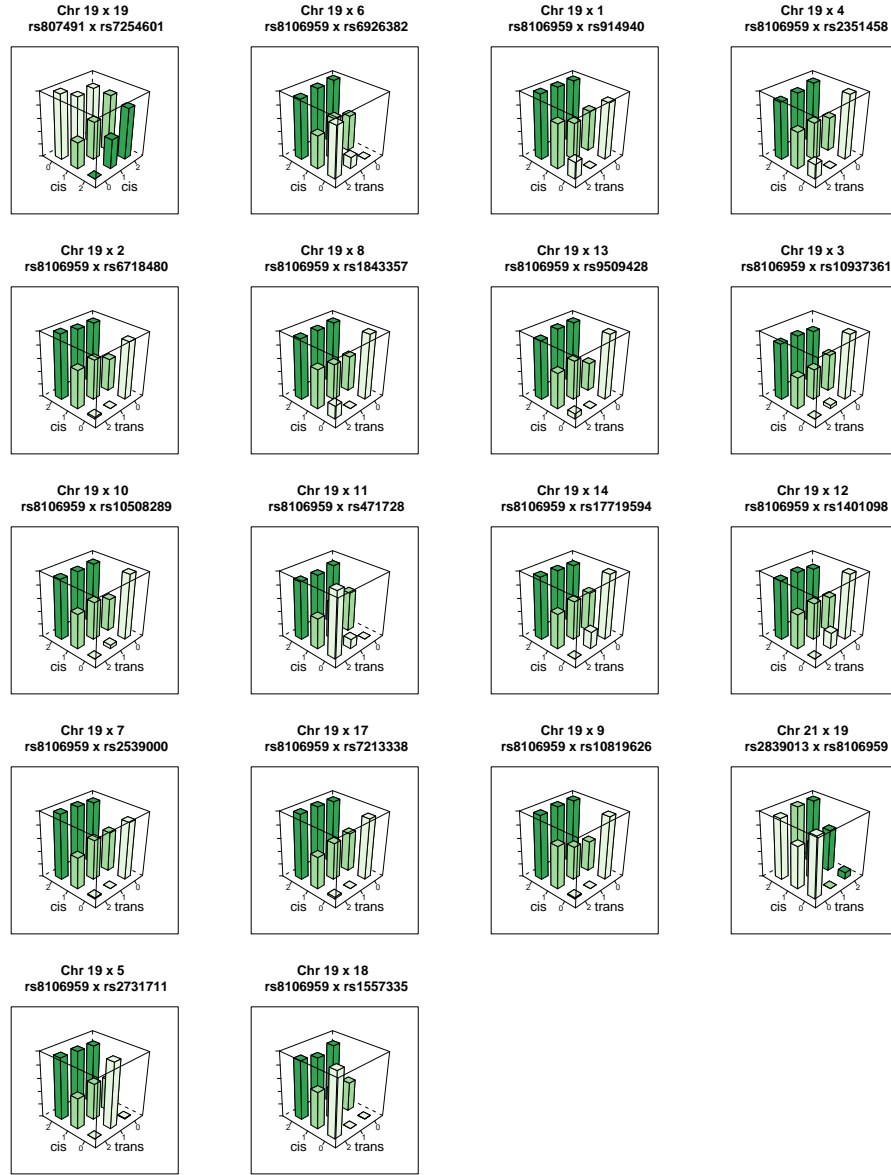


Figure S11: **Genotype-phenotype maps for 19 interactions influencing the expression of TMEM149** Each bar represents the mean phenotypic value for individuals in that genotype class. The rs13069559 SNP typically has a *cis*-additive decreasing effect on the expression of TMEM149, but in many of these interactions the *cis* effect is masked when the *trans* SNP is homozygous for the masking allele.

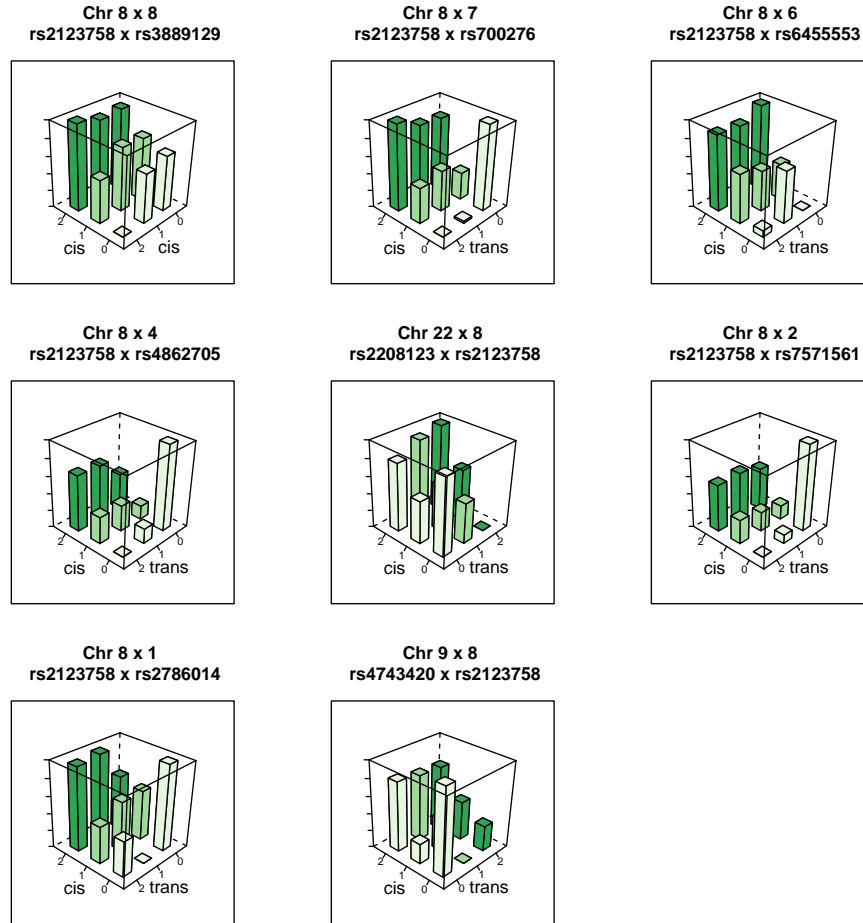


Figure S12: **Genotype-phenotype maps for 8 interactions influencing the expression of NAPRT1** Each bar represents the mean phenotypic value for individuals in that genotype class.

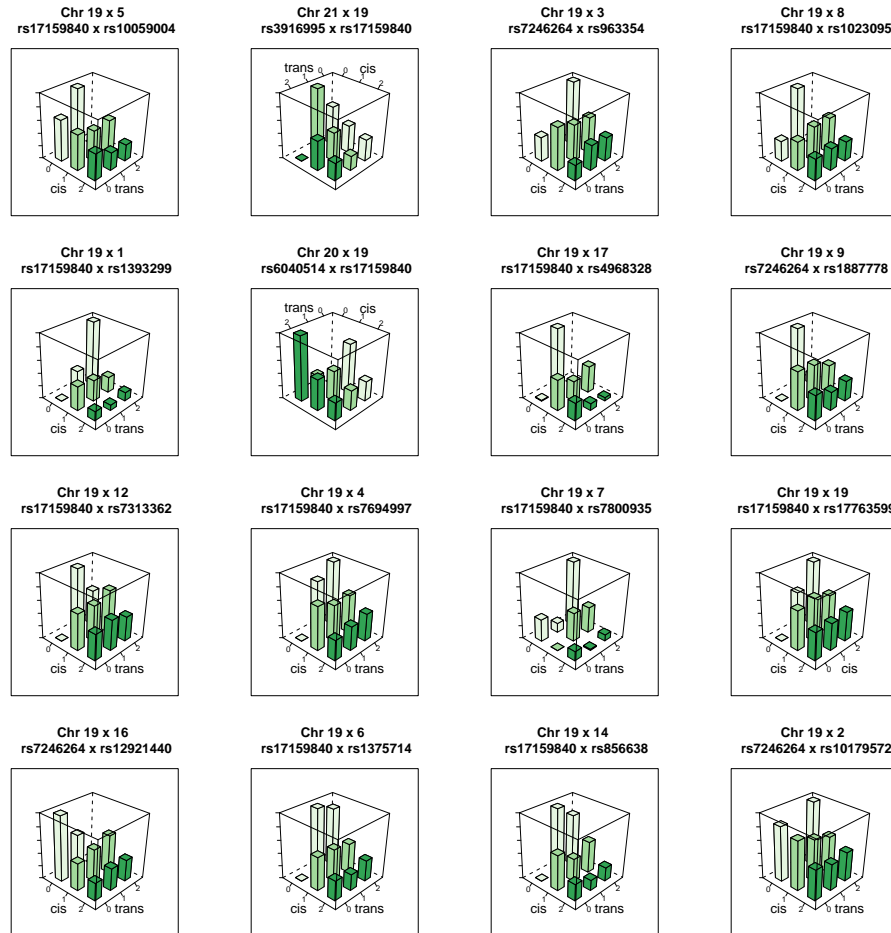


Figure S13: **Genotype-phenotype maps for 16 interactions influencing the expression of TRAPPC5** Each bar represents the mean phenotypic value for individuals in that genotype class.

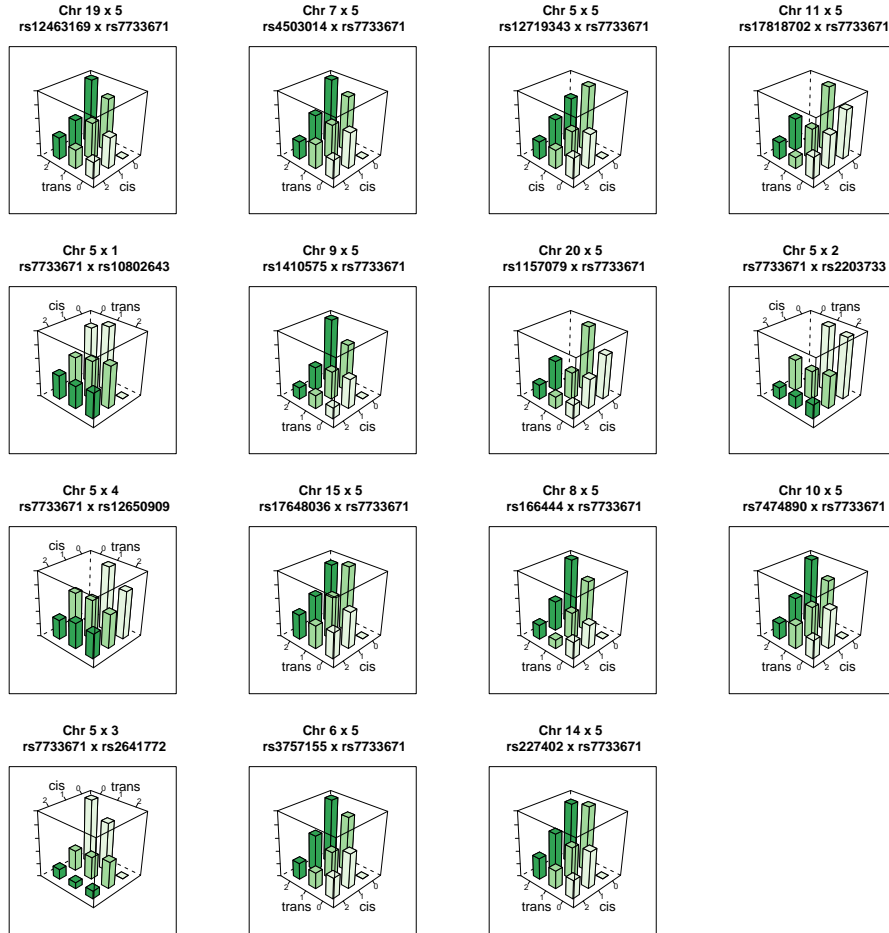


Figure S14: **Genotype-phenotype maps for 15 interactions influencing the expression of CAST** Each bar represents the mean phenotypic value for individuals in that genotype class.

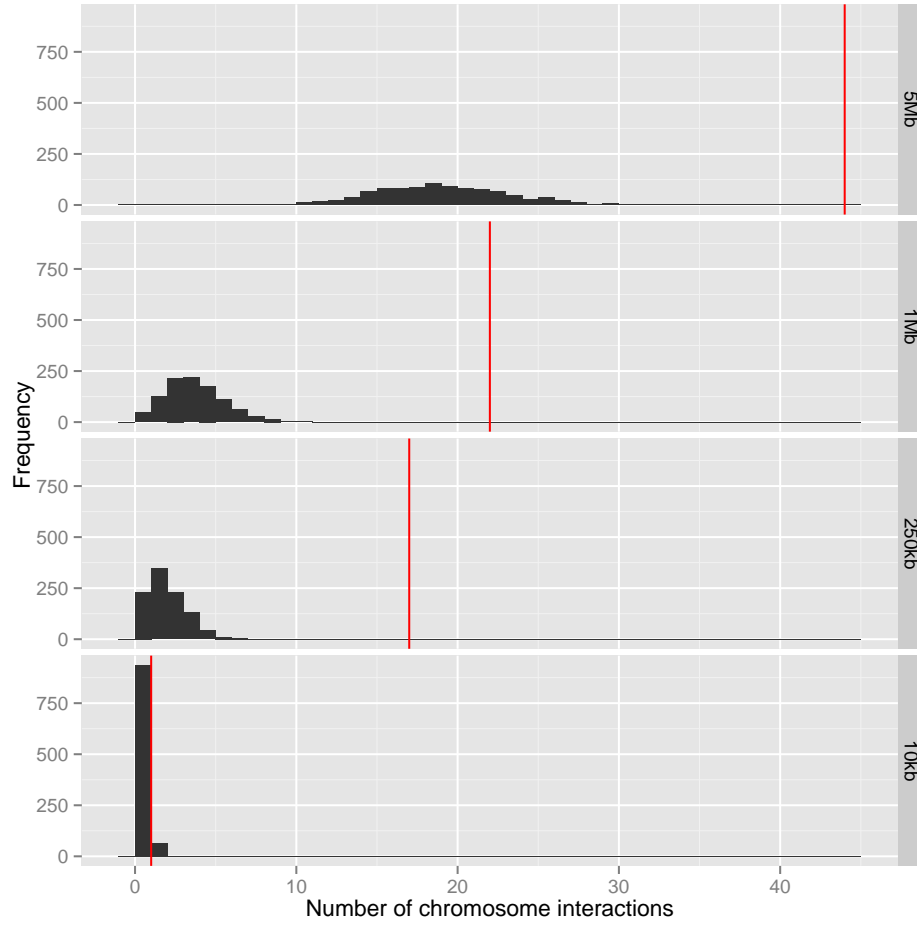


Figure S15: Number of overlaps between chromosome interactions and epistatic interactions Interacting chromosome regions may be a possible mechanism underlying epistatic interactions. The number of epistatic interactions within 20kb, 500kb, 2Mb and 10Mb of known chromosome interacting regions are shown by red vertical lines. The histograms represent the null distribution based on random sampling of 1,000 datasets for each window size.

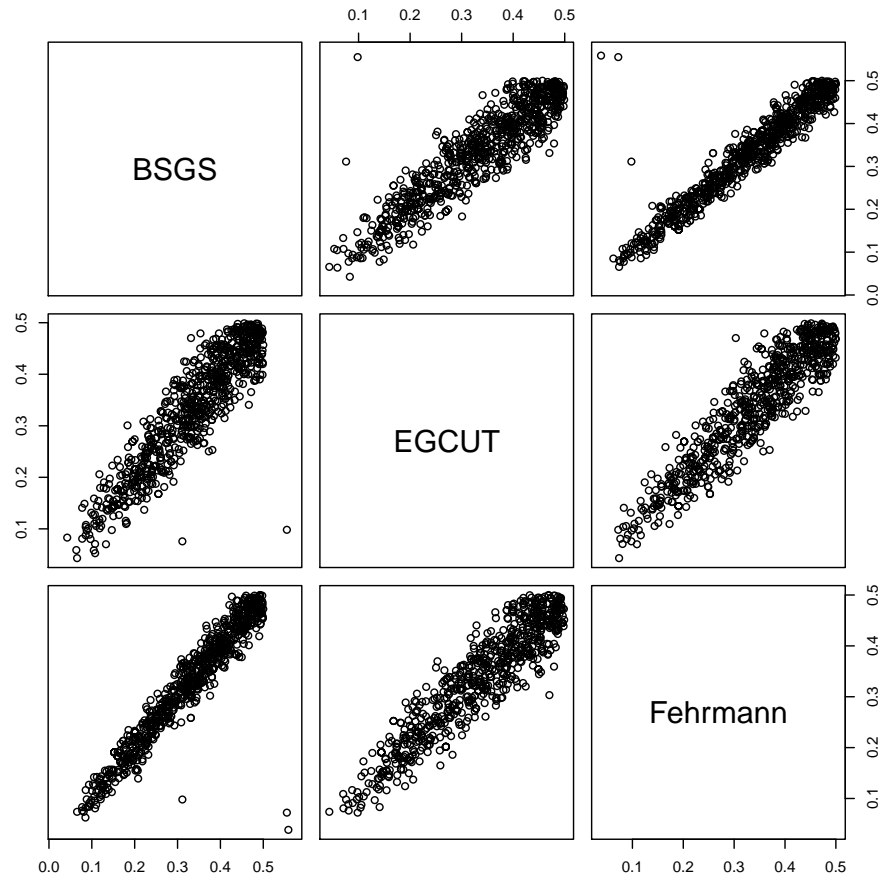


Figure S16: **Comparison of allele frequencies for 781 SNPs involved in genetic interactions across independent populations** Outliers were removed from the analysis as part of the filtering stage during replication.

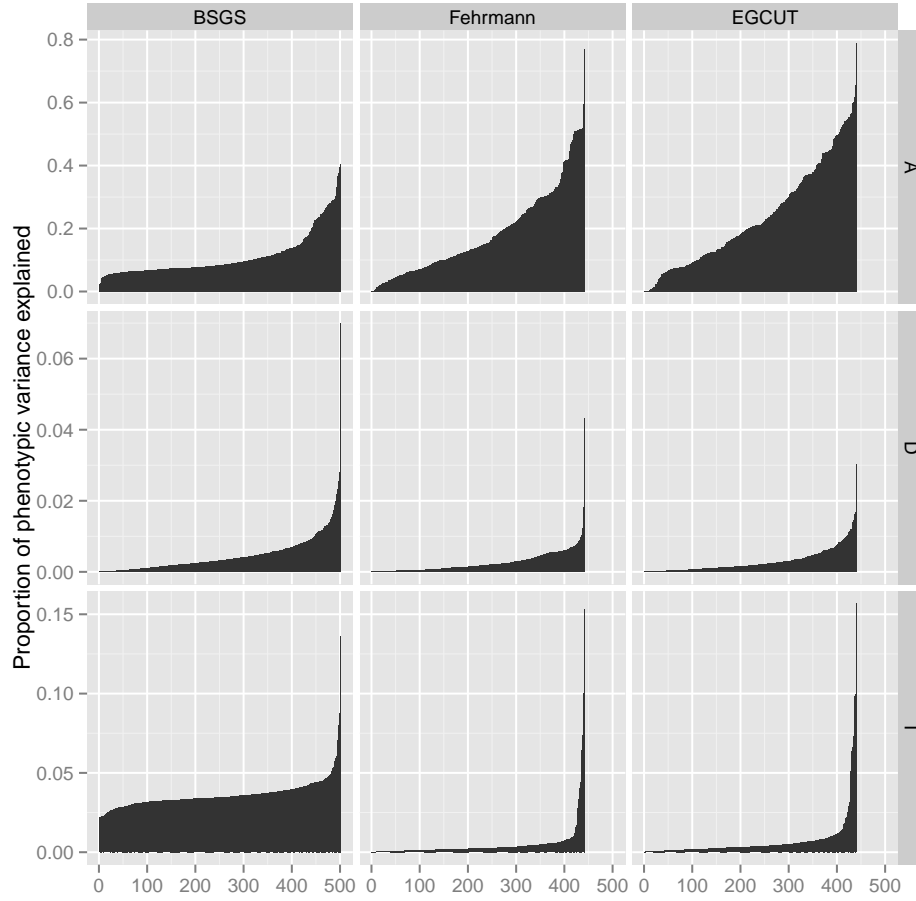


Figure S17: Comparison of variance explained by additive, dominant and epistatic effects from different cohorts How does the estimated variance decomposition change in different cohorts? The proportion of the phenotypic variance that is additive (A), dominant (D), or epistatic (I) for each putative interaction is shown on the y -axis (Note: different scales for each row). BSGS has 501 interactions whereas Fehrmann and EGCUT have 434 (x -axis). The variance estimates in each plot are ordered from lowest additive to highest. This is done independently for each cohort to depict the distribution of estimated effects.

Supplementary Tables

Table S1 – continued from previous page

Expression trait			SNP 1			SNP 2			Interaction statistic / -log ₁₀ p-values			Distance / Mb		
Gene ID ^a	Probe ID ^b	Chr.	rs ID	Chr.	Pos / Mb ^c	Association ^d	rs ID	Chr.	Pos / Mb ^c	Association ^d	BSGS ^e	Fehrmann ^f	EGCUT ^g	Meta ^g
CSORF59	ILMN_1653205	8	rs8051751	16	7188323		rs2896452	8	86102223	CSORF59	5.79	1.39	0.18	0.87
C9ORF72	ILMN_1741881	9	rs10122902	9	27556780	C9ORF72	rs2526698	8	86102223	C9ORF72	6.36	0.96	0.01	0.37
CABO1	ILMN_1731064	10	rs12765847	10	4353908		rs7338725	1	227174210	CABO1	6.36	0.94	0.00	0.34
CARD9	ILMN_1712532	9	rs4266763	9	139289825	INPP5E	rs684040	1	82128660		5.81			
CAST	ILMN_1712532	11	rs4573661	11	6026661		rs4077515	9	139266496	INPP5E	6.61	0.09	0.86	0.42
CAST	ILMN_1717234	19	rs1157079	19	6778978		rs7733671	5	96000269	CAST	7.07	0.23	0.96	0.62
CAST	ILMN_1717234	5	rs12463169	19	17321669		rs7733671	5	96000269	CAST	5.73	0.02	2.85	1.75
CAST	ILMN_1717234	5	rs12599264	16	81840122		rs7733671	5	96000269	CAST	7.00			
CAST	ILMN_1717234	5	rs12719343	5	125369113		rs7733671	5	96000269	CAST	7.68	0.36	1.57	29.369
CAST	ILMN_1717234	5	rs1410575	9	78255630		rs7733671	5	96000269	CAST	6.55	0.13	1.34	0.78
CAST	ILMN_1717234	5	rs166444	8	78392770		rs7733671	5	96000269	CAST	7.01	0.27	0.52	0.37
CAST	ILMN_1717234	5	rs17648036	15	27311111		rs7733671	5	96000269	CAST	7.81	0.97	0.03	0.41
CAST	ILMN_1717234	5	rs17818702	11	86107920		rs7733671	5	96000269	CAST	6.62	1.15	0.59	1.09
CAST	ILMN_1717234	5	rs227402	14	70496867		rs7733671	5	96000269	CAST	6.12	0.11	0.01	0.01
CAST	ILMN_1717234	5	rs2822124	21	15166804		rs7733671	5	96000269	CAST	6.87			
CAST	ILMN_1717234	5	rs3757155	6	136458593		rs7733671	5	96000269	CAST	7.24	0.07	0.33	0.12
CAST	ILMN_1717234	5	rs4503014	7	31149140		rs7733671	5	96000269	CAST	5.88	1.56	1.72	0.92
CAST	ILMN_1717234	5	rs7474890	10	59590078	CAST	rs10802643	1	238120177	CAST	6.74	0.49	0.12	0.23
CAST	ILMN_1717234	5	rs7733671	5	96000269	CAST	rs12650909	4	170128890	CAST	7.42	0.75	0.78	0.93
CAST	ILMN_1717234	5	rs7733671	5	96000269	CAST	rs2203733	2	224093101	CAST	7.42	0.23	0.87	0.50
CAST	ILMN_1717234	5	rs7733671	5	96000269	CAST	rs2641772	3	195531841	CAST	6.07	0.22	0.78	0.54
CAST	ILMN_1651705	11	rs872311	18	66175386		rs11032695	11	634447586	CAT	6.93	0.19	0.26	0.15
CCDC88B	ILMN_1772208	11	rs23532303	19	17099980		rs541207	11	64125142	CCDC88B	5.68	0.33	0.37	0.31
CD86	ILMN_1772208	11	rs694739	17	64097233	CCDC88B	rs12771349	10	96998193		5.62	0.23	0.18	0.14
CD36	ILMN_1784663	7	rs3211834	17	80280117		rs1254900	2	85516334	CD36	6.93	0.15	0.01	0.02
CD93	ILMN_1800540	20	rs1884655	20	23074375	CD93	rs10255470	7	157182030	YAMP8	5.09	0.08	0.03	0.02
CD93	ILMN_1704730	20	rs1884655	20	23074375	CD93	rs4696726	4	7992632	CD93	6.06	1.74	0.24	1.20
CD93	ILMN_1704730	20	rs1884655	20	23074375	CD93	rs7622580	3	196721395	CD93	5.71	0.13	0.80	0.42
CD93	ILMN_1704730	20	rs1884655	20	23074375	CD93	rs838875	12	125145394	CD93	5.56	0.04	0.27	0.08
CD93	ILMN_1704730	20	rs1884655	20	23074375	CD93	rs9576388	13	38434472	CD93	6.31	0.24	1.67	1.16
CD93	ILMN_1704730	20	rs2868504	20	37771578		rs1884655	20	23074375	CD93	5.71	0.71	0.22	0.45
CD93	ILMN_1704730	20	rs4813479	20	23076914	CD93	rs10925747	1	238899903	CD93	7.43			
CD93	ILMN_1704730	20	rs4813479	20	23076914	CD93	rs2873420	8	136500554	CD93	7.02			
CD93	ILMN_1704730	20	rs4813479	20	23076914	CD93	rs428531	18	74439542	CD93	6.13			
CD93	ILMN_1704730	20	rs4813479	20	23076914	CD93	rs4789891	17	77264482	CD93	6.08			
CD93	ILMN_1704730	20	rs861544	14	104162263		rs7324744	13	115008038	CD93	5.46	0.21	0.14	0.11
CDK5R1	ILMN_2339796	13	rs9905940	17	46614102	HOXB2	rs11655031	17	30831362	CDK5R1	5.47	0.95	0.07	0.45
CEACAM21	ILMN_1745949	19	rs200690	19	51956250	CEACAM21	rs4803481	19	42068556	CEACAM21	6.15	0.90	0.12	0.48
CEACAM21	ILMN_1745949	19	rs4803481	19	42068556	CEACAM21	rs2421050	5	158943044	CEACAM21	6.67	2.16	0.16	1.44
CEP102	ILMN_1703754	18	rs6505780	18	13069782	CEP102	rs13132719	4	180265266	CEP102	5.75	0.15	0.24	0.12
CEP63	ILMN_1787808	3	rs3282569	14	101350298		rs13079012	3	134247706	ANAPC13	6.36	0.23	0.10	0.09
CES1	ILMN_2359945	16	rs8192935	16	55861794	CES1	rs772788	2	235248562	CES1	5.65			
CHPT1	ILMN_2209240	12	rs591967	13	38831922		rs2695290	12	102087844	CHPT1	5.74	0.72	0.20	0.44
CHPT1	ILMN_2209240	12	rs6539014	12	102277782		rs867578	11	81937002	CHPT1	4.75	0.92	0.02	0.36
CLEC12A	ILMN_1663142	12	rs429790	16	84471642		rs7313235	12	10132283	CLEC12A	5.55	0.07	1.28	0.67
CLEC12A	ILMN_2403228	12	rs7305054	11	96929337		rs3903088	10	134236688	CLEC12A	7.54	0.95	0.36	0.73
CLTB	ILMN_1674609	5	rs17129799	11	96929337		rs6863172	5	173595960	CLTB	5.55	0.27	0.07	0.02
CNN2	ILMN_1770290	19	rs3752237	19	1047161	ABCA7	rs169130	16	63121080	CNN2	7.56	0.07	0.28	1.39
CPFL	ILMN_1654545	8	rs4333645	8	145569535	ABCA7	rs7736017	13	67713633	CPFL	6.33	1.92	0.01	0.01
CPVL	ILMN_1682928	7	rs12596791	16	26115562		rs2455884	4	61738094	CPVL	5.74	0.06	0.57	0.23

Continued on next page

Table S1 – continued from previous page

Gene ID ^a	Expression trait	Probe ID ^b		SNP 1			SNP 2			BSGS ^e	Interaction statistic ^f / -log ₁₀ p-values	MetaSig ^g	Distance / Mb ^h	
		Chr.	rs ID	Chr.	Pos/Mb ^c	Association ^d	rs ID	Chr.	Pos/Mb ^c					Association ^d
CPVL	ILMN-1682928	7	rs2835998	21	39202070		rs2835884	7	29188475	CPVL	5.55	0.19	0.03	0.04
CRPT	ILMN-1813256	20	rs2131290	4	188859908		rs1531133	2	46843651	CRPT	5.47	0.28	0.10	0.12
CRPT	ILMN-1737685	2	rs6139887	20	5986234	CRUS1	rs1473927	5	62406408		6.18	0.10	0.36	0.15
CTSC	ILMN-1707197	18	rs9979356	21	432500974		rs3761385	21	15198355	CTSC	11.99	23.20	16.72	42.27
CTSC	ILMN-1804834	18	rs9249438	18	692009305		rs1763882	5	138246767	CTSC	5.74	0.02	0.41	0.11
	ILMN-1606347	11	rs4257584	11	8859983		rs10793264	10	108619632	CTSC	7.16	0.92	0.44	0.37
CTSC	ILMN-2242463	22	rs1815387	22	2955555		rs5568912	11	89077352	CTSC	7.16	0.92	0.44	0.37
CTSC	ILMN-2242463	11	rs7049237	22	88117965		rs5568912	11	89077352	CTSC	7.16	18.76	15.06	33.53
CWFL9L1	ILMN-1651886	11	rs108734	11	11456927		rs12784396	10	102027407	CWFL9L1	5.42	0.21	0.01	0.03
CYBRD1	ILMN-1711896	10	rs2502948	4	129994690		rs888427	2	172368120	CYBRD1	5.89	0.23	0.53	0.34
CYBRD1	ILMN-1712305	2	rs7852475	9	14698856		rs888427	2	172368120	CYBRD1	5.68	0.20	0.02	0.04
CYBRD1	ILMN-1726792	2	rs11257679	10	12318294		rs888427	2	172368120	CYBRD1	5.81	0.39	1.87	1.47
CYBRD1	ILMN-2087692	2	rs6137908	20	23344590		rs888427	2	172368120	CYBRD1	5.85	0.05	0.83	0.36
CYBRD1	ILMN-2087692	2	rs888427	20	23344590	CYBRD1	rs7591849	2	160112881		5.85	0.87	0.10	0.44
CYP27A1	ILMN-1704985	2	rs6021982	20	36571928		rs933994	2	219650616	CYP27A1	5.42	0.29	0.86	0.60
DAB2	ILMN-1728428	5	rs7778910	7	110451383		rs835223	3	39381357	DAB2	5.44	0.48	0.41	0.44
DDT	ILMN-1811648	17	rs9900173	17	43111688	DDT	rs1343244	6	82076988		9.12	0.00	0.58	0.14
DDT	ILMN-1690982	22	rs5760102	22	2448761		rs2378341	3	187475208	DDT	5.62	0.64	0.05	0.42
DDX5	ILMN-1797001	9	rs4937097	11	125962645		rs7042042	9	32451144	DDX5	5.31	0.61	0.29	0.41
DEM1	ILMN-1783996	11	rs10120023	11	106703727	COQ10A	rs2519515	7	88204888		5.47	0.08	0.41	0.16
DEM1	ILMN-1783996	11	rs12363827	11	106703727		rs10120023	9	137810259	COQ10A	6.39	0.77	0.02	0.29
DEM1	ILMN-1783996	11	rs1519956	12	89468283		rs7566044	2	169960422	DEM1	6.00	0.06	1.17	0.58
DHRS9	ILMN-1733998	8	rs1528529	7	147132505		rs7566044	2	169960422	DHRS9	6.48	0.37	0.34	0.32
DHRS9	ILMN-2384181	21	rs2831914	21	29959453		rs2161037	2	169893419	DHRS9	5.51	0.88	0.04	0.37
DHRS9	ILMN-2384181	21	rs7661304	4	187776431		rs2161037	2	169893419	DHRS9	7.64	0.05	0.11	0.03
DIP2B	ILMN-1755589	12	rs1080134	17	29161503		rs11169322	12	50610976	DIP2B	4.65	0.32	0.05	0.10
DIP2B	ILMN-1755589	12	rs169335	12	50636364	LASS5	rs2872008	7	153134888		4.87	0.30	0.58	
DIP2B	ILMN-1755589	12	rs338585	19	41711815		rs7134595	12	50730458	DIP2B	5.31	50730458	0.22	0.19
DIP2B	ILMN-1755589	12	rs134595	12	50730458	LASS5	rs1808634	8	61971140		4.40	0.37		
DIP2B	ILMN-1755589	12	rs7312552	12	50744171	LASS5	rs4532958	10	115214154	DIP2B	5.03	0.09	0.02	0.01
DIP2B	ILMN-1755589	12	rs871257	12	50744171	LASS5	rs4532958	10	115214154	DIP2B	5.92	0.48	0.00	0.11
DIP2B	ILMN-1755589	12	rs871257	12	50744171	LASS5	rs4532958	10	115214154	DIP2B	5.92	0.48	0.00	0.11
DIP2B	ILMN-1755589	12	rs871257	12	50744171	LASS5	rs4532958	10	115214154	DIP2B	5.92	0.48	0.00	0.11
DIP2B	ILMN-1755589	12	rs871257	12	50744171	LASS5	rs4532958	10	115214154	DIP2B	5.92	0.48	0.00	0.11
DIP2B	ILMN-1755589	12	rs871257	12	50744171	LASS5	rs4532958	10	115214154	DIP2B	5.92	0.48	0.00	0.11
DIP2B	ILMN-1755589	12	rs871257	12	50744171	LASS5	rs4532958	10	115214154	DIP2B	5.92	0.48	0.00	0.11
DIP2B	ILMN-1755589	12	rs871257	12	50744171	LASS5	rs4532958	10	115214154	DIP2B	5.92	0.48	0.00	0.11
DIP2B	ILMN-1755589	12	rs871257	12	50744171	LASS5	rs4532958	10	115214154	DIP2B	5.92	0.48	0.00	0.11
DIP2B	ILMN-1755589	12	rs871257	12	50744171	LASS5	rs4532958	10	115214154	DIP2B	5.92	0.48	0.00	0.11
DIP2B	ILMN-1755589	12	rs871257	12	50744171	LASS5	rs4532958	10	115214154	DIP2B	5.92	0.48	0.00	0.11
DIP2B	ILMN-1755589	12	rs871257	12	50744171	LASS5	rs4532958	10	115214154	DIP2B	5.92	0.48	0.00	0.11
DIP2B	ILMN-1755589	12	rs871257	12	50744171	LASS5	rs4532958	10	115214154	DIP2B	5.92	0.48	0.00	0.11
DIP2B	ILMN-1755589	12	rs871257	12	50744171	LASS5	rs4532958	10	115214154	DIP2B	5.92	0.48	0.00	0.11
DIP2B	ILMN-1755589	12	rs871257	12	50744171	LASS5	rs4532958	10	115214154	DIP2B	5.92	0.48	0.00	0.11
DIP2B	ILMN-1755589	12	rs871257	12	50744171	LASS5	rs4532958	10	115214154	DIP2B	5.92	0.48	0.00	0.11
DIP2B	ILMN-1755589	12	rs871257	12	50744171	LASS5	rs4532958	10	115214154	DIP2B	5.92	0.48	0.00	0.11
DIP2B	ILMN-1755589	12	rs871257	12	50744171	LASS5	rs4532958	10	115214154	DIP2B	5.92	0.48	0.00	0.11
DIP2B	ILMN-1755589	12	rs871257	12	50744171	LASS5	rs4532958	10	115214154	DIP2B	5.92	0.48	0.00	0.11
DIP2B	ILMN-1755589	12	rs871257	12	50744171	LASS5	rs4532958	10	115214154	DIP2B	5.92	0.48	0.00	0.11
DIP2B	ILMN-1755589	12	rs871257	12	50744171	LASS5	rs4532958	10	115214154	DIP2B	5.92	0.48	0.00	0.11
DIP2B	ILMN-1755589	12	rs871257	12	50744171	LASS5	rs4532958	10	115214154	DIP2B	5.92	0.48	0.00	0.11
DIP2B	ILMN-1755589	12	rs871257	12	50744171	LASS5	rs4532958	10	115214154	DIP2B	5.92	0.48	0.00	0.11
DIP2B	ILMN-1755589	12	rs871257	12	50744171	LASS5	rs4532958	10	115214154	DIP2B	5.92	0.48	0.00	0.11
DIP2B	ILMN-1755589	12	rs871257	12	50744171	LASS5	rs4532958	10	115214154	DIP2B	5.92	0.48	0.00	0.11
DIP2B	ILMN-1755589	12	rs871257	12	50744171	LASS5	rs4532958	10	115214154	DIP2B	5.92	0.48	0.00	0.11
DIP2B	ILMN-1755589	12	rs871257	12	50744171	LASS5	rs4532958	10	115214154	DIP2B	5.92	0.48	0.00	0.11
DIP2B	ILMN-1755589	12	rs871257	12	50744171	LASS5	rs4532958	10	115214154	DIP2B	5.92	0.48	0.00	0.11
DIP2B	ILMN-1755589	12	rs871257	12	50744171	LASS5	rs4532958	10	115214154	DIP2B	5.92	0.48	0.00	0.11
DIP2B	ILMN-1755589	12	rs871257	12	50744171	LASS5	rs4532958	10	115214154	DIP2B	5.92	0.48	0.00	0.11
DIP2B	ILMN-1755589	12	rs871257	12	50744171	LASS5	rs4532958	10	115214154	DIP2B	5.92	0.48	0.00	0.11
DIP2B	ILMN-1755589	12	rs871257	12	50744171	LASS5	rs4532958	10	115214154	DIP2B	5.92	0.48	0.00	0.11
DIP2B	ILMN-1755589	12	rs871257	12	5074417									

0.23 Continued on next page

Table S1 – continued from previous page

Gene ID ^a	Expression trait	Chr.	rs ID	Chr.	SNP 1	Pos/Mb ^c	Association ^d	rs ID	Chr.	SNP 2	Pos/Mb ^c	Association ^d	BSGS ^e	Interaction statistic ^f	-log ₁₀ p-values	EGCUT	Meta ^g	Distance / Mb ^b
HBG2	ILMN.2084825	11	rs12975066	19	37233501		HBG2	rs2855039	11	5271671		HBG2	5.77	0.08	0.13	0.05		
HBG2	ILMN.2084825	11	rs2855039	11	5271671		HBG2	rs12042181	1	213085494		HBG2	6.84	0.06	0.34	0.21		
HBG2	ILMN.2084825	11	rs2855039	11	5271671		HBG2	rs12053379	4	141533832		HBG2	5.98	0.00	0.46	0.10		
HBG7	ILMN.18602186	12	rs2109029	16	6036851		HBG7	rs17606036	12	48173352		HBG7	5.75	0.15	0.59	0.32		
HEBP1	ILMN.18602587	12	rs3782507	12	13145013		HEBP1	rs176860635	17	1332200622		HEBP1	5.98	0.00	0.59	0.32		
HEBP1	ILMN.18602587	12	rs3782507	12	13145013		HEBP1	rs176860635	17	1332200622		HEBP1	5.98	0.00	0.59	0.32		
HEBP1	ILMN.18602587	12	rs3782507	12	13145013		HEBP1	rs176860635	17	1332200622		HEBP1	5.98	0.00	0.59	0.32		
HEBP1	ILMN.18602587	12	rs3782507	12	13145013		HEBP1	rs176860635	17	1332200622		HEBP1	5.98	0.00	0.59	0.32		
HEBP1	ILMN.18602587	12	rs3782507	12	13145013		HEBP1	rs176860635	17	1332200622		HEBP1	5.98	0.00	0.59	0.32		
HEBP1	ILMN.18602587	12	rs3782507	12	13145013		HEBP1	rs176860635	17	1332200622		HEBP1	5.98	0.00	0.59	0.32		
HEBP1	ILMN.18602587	12	rs3782507	12	13145013		HEBP1	rs176860635	17	1332200622		HEBP1	5.98	0.00	0.59	0.32		
HEBP1	ILMN.18602587	12	rs3782507	12	13145013		HEBP1	rs176860635	17	1332200622		HEBP1	5.98	0.00	0.59	0.32		
HEBP1	ILMN.18602587	12	rs3782507	12	13145013		HEBP1	rs176860635	17	1332200622		HEBP1	5.98	0.00	0.59	0.32		
HEBP1	ILMN.18602587	12	rs3782507	12	13145013		HEBP1	rs176860635	17	1332200622		HEBP1	5.98	0.00	0.59	0.32		
HEBP1	ILMN.18602587	12	rs3782507	12	13145013		HEBP1	rs176860635	17	1332200622		HEBP1	5.98	0.00	0.59	0.32		
HEBP1	ILMN.18602587	12	rs3782507	12	13145013		HEBP1	rs176860635	17	1332200622		HEBP1	5.98	0.00	0.59	0.32		
HEBP1	ILMN.18602587	12	rs3782507	12	13145013		HEBP1	rs176860635	17	1332200622		HEBP1	5.98	0.00	0.59	0.32		
HEBP1	ILMN.18602587	12	rs3782507	12	13145013		HEBP1	rs176860635	17	1332200622		HEBP1	5.98	0.00	0.59	0.32		
HEBP1	ILMN.18602587	12	rs3782507	12	13145013		HEBP1	rs176860635	17	1332200622		HEBP1	5.98	0.00	0.59	0.32		
HEBP1	ILMN.18602587	12	rs3782507	12	13145013		HEBP1	rs176860635	17	1332200622		HEBP1	5.98	0.00	0.59	0.32		
HEBP1	ILMN.18602587	12	rs3782507	12	13145013		HEBP1	rs176860635	17	1332200622		HEBP1	5.98	0.00	0.59	0.32		
HEBP1	ILMN.18602587	12	rs3782507	12	13145013		HEBP1	rs176860635	17	1332200622		HEBP1	5.98	0.00	0.59	0.32		
HEBP1	ILMN.18602587	12	rs3782507	12	13145013		HEBP1	rs176860635	17	1332200622		HEBP1	5.98	0.00	0.59	0.32		
HEBP1	ILMN.18602587	12	rs3782507	12	13145013		HEBP1	rs176860635	17	1332200622		HEBP1	5.98	0.00	0.59	0.32		
HEBP1	ILMN.18602587	12	rs3782507	12	13145013		HEBP1	rs176860635	17	1332200622		HEBP1	5.98	0.00	0.59	0.32		
HEBP1	ILMN.18602587	12	rs3782507	12	13145013		HEBP1	rs176860635	17	1332200622		HEBP1	5.98	0.00	0.59	0.32		
HEBP1	ILMN.18602587	12	rs3782507	12	13145013		HEBP1	rs176860635	17	1332200622		HEBP1	5.98	0.00	0.59	0.32		
HEBP1	ILMN.18602587	12	rs3782507	12	13145013		HEBP1	rs176860635	17	1332200622		HEBP1	5.98	0.00	0.59	0.32		
HEBP1	ILMN.18602587	12	rs3782507	12	13145013		HEBP1	rs176860635	17	1332200622		HEBP1	5.98	0.00	0.59	0.32		
HEBP1	ILMN.18602587	12	rs3782507	12	13145013		HEBP1	rs176860635	17	1332200622		HEBP1	5.98	0.00	0.59	0.32		
HEBP1	ILMN.18602587	12	rs3782507	12	13145013		HEBP1	rs176860635	17	1332200622		HEBP1	5.98	0.00	0.59	0.32		
HEBP1	ILMN.18602587	12	rs3782507	12	13145013		HEBP1	rs176860635	17	1332200622		HEBP1	5.98	0.00	0.59	0.32		
HEBP1	ILMN.18602587	12	rs3782507	12	13145013		HEBP1	rs176860635	17	1332200622		HEBP1	5.98	0.00	0.59	0.32		
HEBP1	ILMN.18602587	12	rs3782507	12	13145013		HEBP1	rs176860635	17	1332200622		HEBP1	5.98	0.00	0.59	0.32		
HEBP1	ILMN.18602587	12	rs3782507	12	13145013		HEBP1	rs176860635	17	1332200622		HEBP1	5.98	0.00	0.59	0.32		
HEBP1	ILMN.18602587	12	rs3782507	12	13145013		HEBP1	rs176860635	17	1332200622		HEBP1	5.98	0.00	0.59	0.32		
HEBP1	ILMN.18602587	12	rs3782507	12	13145013		HEBP1	rs176860635	17	1332200622		HEBP1	5.98	0.00	0.59	0.32		
HEBP1	ILMN.18602587	12	rs3782507	12	13145013		HEBP1	rs176860635	17	1332200622		HEBP1	5.98	0.00	0.59	0.32		
HEBP1	ILMN.18602587	12	rs3782507	12	13145013		HEBP1	rs176860635	17	1332200622		HEBP1	5.98	0.00	0.59	0.32		
HEBP1	ILMN.18602587	12	rs3782507	12	13145013		HEBP1	rs176860635	17	1332200622		HEBP1	5.98	0.00	0.59	0.32		
HEBP1	ILMN.18602587	12	rs3782507	12	13145013		HEBP1	rs176860635	17	1332200622		HEBP1	5.98	0.00	0.59	0.32		
HEBP1	ILMN.18602587	12	rs3782507	12	13145013		HEBP1	rs176860635	17	1332200622		HEBP1	5.98	0.00	0.59	0.32		
HEBP1	ILMN.18602587	12	rs3782507	12	13145013		HEBP1	rs176860635	17	1332200622		HEBP1	5.98	0.00	0.59	0.32		
HEBP1	ILMN.18602587	12	rs3782507	12	13145013		HEBP1	rs176860635	17	1332200622		HEBP1	5.98	0.00	0.59	0.32		
HEBP1	ILMN.18602587	12	rs3782507	12	13145013		HEBP1	rs176860635	17	1332200622		HEBP1	5.98	0.00	0.59	0.32		
HEBP1	ILMN.18602587	12	rs3782507	12	13145013		HEBP1	rs176860635	17	1332200622		HEBP1	5.98	0.00	0.59	0.32		
HEBP1	ILMN.18602587	12	rs3782507	12	13145013		HEBP1	rs176860635	17	1332200622		HEBP1	5.98	0.00	0.59	0.32		
HEBP1	ILMN.18602587	12	rs3782507	12	13145013		HEBP1	rs176860635	17	1332200622		HEBP1	5.98	0.00	0.59	0.32		
HEBP1	ILMN.18602587	12	rs3782507	12	13145013		HEBP1	rs176860635	17	1332200622		HEBP1	5.98	0.00	0.59	0.32		
HEBP1	ILMN.18602587	12	rs3782507	12	13145013		HEBP1	rs176860635	17	1332200622		HEBP1	5.98	0.00	0.59	0.32		
HEBP1	ILMN.18602587	12	rs3782507	12	13145013		HEBP1	rs176860635	17	1332200622		HEBP1	5.98	0.00	0.59	0.32		
HEBP1	ILMN.18602587	12	rs3782507	12	13145013		HEBP1	rs176860635	17	1332200622		HEBP1	5.98	0.00	0.59	0.32		
HEBP1	ILMN.18602587	12	rs3782507	12	13145013		HEBP1	rs176860635	17	1332200622		HEBP1	5.98	0.00	0.59	0.32		
HEBP1	ILMN.18602587	12	rs3782507	12	13145013		HEBP1	rs176860635	17	1332200622		HEBP1	5.98	0.00	0.59	0.32		
HEBP1	ILMN.18602587	12	rs3782507	12	13145013		HEBP1	rs176860635	17	1332200622		HEBP1	5.98	0.00	0.59	0.32		
HEBP1	ILMN.18602587	12	rs3782507	12	13145013		HEBP1	rs176860635	17	1332200622		HEBP1	5.98	0.00	0.59	0.32		
HEBP1	ILMN.18602587	12	rs3782507	12	13145013		HEBP1	rs176860635	17	1332200622		HEBP1	5.98	0.00	0.59	0.32		
HEBP1	ILMN.18602587	12	rs3782507	12	13145013		HEBP1	rs176860635	17	1332200622		HEBP1	5.98	0.00	0.59	0.32		
HEBP1	ILMN.18602587	12	rs3782507	12	13145013		HEBP1	rs176860635	17	1332200622		HEBP1	5.98	0.00	0.59	0.32		
HEBP1	ILMN.18602587	12	rs3782507	12	13145013		HEBP1	rs176860635	17	1332200622		HEBP1	5.98	0.00	0.59	0.32		
HEBP1	ILMN.18602587	12	rs3782507	12	13145013		HEBP1	rs176860635	17	1332200622		HEBP1	5.98	0.00	0.59	0.32		
HEBP1	ILMN.18602587	12	rs3782507	12	13145013		HEBP1	rs176860635	17	1332200622		HEBP1	5.98	0.00	0.59	0.32		
HEBP1	ILMN.18602587	12	rs3782507	12	13145013		HEBP1	rs176860635	17	1332200622		HEBP1	5.98	0.00	0.59	0.32		
HEBP1	ILMN.18602587	12	rs3782507	12	13145013		HEBP1	rs176860635	17	1332200622		HEBP1	5.98	0.00	0.59	0.32		
HEBP1	ILMN.18602587	12	rs3782507	12	13145013		HEBP1	rs176860635	17	1332200622		HEBP1	5.98	0.00	0.59	0.32		
HEBP1	ILMN.18602587	12	rs3782507	12	13145013		HEBP1	rs176860635	17	1332200622		HEBP1	5.98	0.00	0.59	0.32		
HEBP1	ILMN.18602587	12	rs3782507	12	13145013		HEBP1	rs176860635	17	1332200622		HEBP1	5.98	0.00	0.59	0.32		
HEBP1	ILMN.18602587	12	rs3782507	12	13145013		HEBP1	rs176860635	17	1332200622		HEBP1	5.98	0.00	0.59	0.32		
HEBP1	ILMN.18602587	12	rs3782507	12	13145013		HEBP1	rs176860635	17	1332200622		HEBP1	5.98	0.00	0.59	0.32		
HEBP1	ILMN.18602587	12	rs3782507	12	13145013		HEBP1	rs176860635	17	1332200622		HEBP1	5.98	0.00	0.59	0.32		
HEBP1	ILMN.18602587	12	rs3782507	12	13145013		HEBP1	rs176860635	17									

3.30 Continued on next page

Table S1 – continued from previous page

[illegible]

Continued on next page

Table S1 – continued from previous page

Gene ID ^a	Expression trait	SNP 1			SNP 2			Interaction statistic / -log ₁₀ p-values				Distance / Mb ^b	
		rs ID	Chr.	Pos/Mb ^c	Association ^d	rs ID	Chr.	Pos/Mb ^c	Association ^d	BSGS ^e	Fehrmann ^f		EGCUT ^g
NRBF2	ILMN-3237385	rs6025645	20	56157341		rs7923609	10	65133822	NRBF2	5.45			
NRBF2	ILMN-3237385	rs6017815	21	19819016		rs7923609	10	65133822	NRBF2	6.11	0.47	0.05	0.17
NRD1	ILMN-1800897	rs4852124	2	240680022		rs6588415	1	52334047	NRBF2	6.13	0.03	0.46	0.13
NUDT18	ILMN-1787885	rs5017351	11	25453442		rs1005901	8	21964378	NUDT18	5.44	4.27	1.35	9.03
OAS1	ILMN-1658247	rs11613438	12	113480510		rs1047944	6	163997467		8.59	0.43	0.81	3.86
OAS1	ILMN-1658247	rs113311	12	113480510		rs2072133	12	113409260		4.13	4.12	0.81	3.86
OAS1	ILMN-1675640	rs2892233	19	49160255		rs3741981	12	13169066	OAS1	4.38	0.87	0.46	0.14
OPTN	ILMN-2381899	rs7192613	16	74286646		rs17312962	10	13169066	OPTN	5.64	0.42	0.06	0.14
OSBPL5	ILMN-2307032	rs2829679	21	26625433		rs998639	11	3149249	OSBPL5	5.00	0.36	0.00	0.07
OSTF1	ILMN-1742456	rs17780195	9	77755469		rs2273770	9	77755469	OSTF1	5.42	0.16	0.87	0.49
OSTF1	ILMN-1742456	rs2273770	9	77755469	OSTF1	rs7775469	9	77755469	OSTF1	5.42	1.20	0.08	0.62
OVGP1	ILMN-1734542	rs10802822	1	240132968		rs1264898	5	119928923	OVGP1	5.43	0.13	1.48	0.88
OVGP1	ILMN-1734542	rs347351	3	140148107		rs1264894	1	111969719	OVGP1	6.04	0.25	1.21	0.82
PAM	ILMN-2313901	rs28092	5	102149795	PAM	rs7846000	1	40139553	HPCAL4	5.59	0.66	0.44	0.59
PCYOX1L	ILMN-1815951	rs24358490	5	14826162	PCYOX1L	rs2731939	3	21395989		6.20	0.19	0.26	0.16
PRX5	ILMN-1660232	rs10444467	12	128052636		rs4328748	12	7364442	PEX5	5.85	0.09	0.71	0.32
PRX5	ILMN-1660232	rs7495797	15	27246462		rs4328748	12	7364442	PEX5	5.74	0.34	0.09	0.13
PFAAP5	ILMN-1797893	rs131969	22	49151303		rs1263806	14	21982957	PFAAP5	5.64	0.87	0.36	0.67
PGLYRP1	ILMN-1704870	rs12982353	19	46529456		rs10736812	11	76708066	PHCA	5.51	0.03	0.65	0.24
PHCA	ILMN-1812552	rs495642	11	123097386		rs2065841	1	61728597	PHCA	5.90	0.36	0.90	0.70
PIK3P1	ILMN-1719986	rs4141404	22	31675185	PIK3P1	rs10498313	14	30398876		5.23	0.20	0.01	0.03
PISD	ILMN-1739934	rs615752	22	33233431	PISD	rs1465754	22	32097775		7.11	0.00	1.19	0.48
PISD	ILMN-1739934	rs715572	22	33233431		rs6518754	22	32097775	PISD	4.12	0.05	0.42	0.15
PNKD	ILMN-1774604	rs6869411	9	45871604		rs928046	9	140487108	PNKD	6.35	0.16	0.04	0.04
PNPLA7	ILMN-1662587	rs910119	20	48668255		rs4758001	11	17569830	PNPLA7	5.15	0.31	0.78	0.56
PPFIBP2	ILMN-1662587	rs1293103	15	58308096		rs1156875	14	35619816	PPFIBP2	4.44	0.29	0.33	0.26
PP2R5A	ILMN-1738784	rs10930170	2	163999467		rs12120009	1	212447167	PP2R5A	5.81	0.12	0.42	0.19
PP2R5A	ILMN-1738784	rs124243255	12	123595064		rs12120009	1	212447167	PP2R5A	5.63	0.72	0.48	0.66
PP2R5A	ILMN-1738784	rs1889083	13	66222691		rs12120009	1	212447167	PP2R5A	5.72	0.08	0.95	0.46
PP2R5A	ILMN-1738784	rs6822334	1	107417238		rs12120009	1	212447167	PP2R5A	5.61	0.36	0.13	0.17
PP2R5A	ILMN-1738784	rs7757871	6	135030045		rs12120009	1	212447167	PP2R5A	5.65	1.69	0.28	1.21
PP2R5A	ILMN-1738784	rs7871178	9	27148475		rs12120009	1	212447167	PP2R5A	5.95	0.37	0.06	0.12
PRDX5	ILMN-1716063	rs8019823	16	95040482		rs11600990	11	64082807	PP2R5A	5.72	0.16	0.30	0.16
PRKCB1	ILMN-1716063	rs2188355	16	23867776		rs10492793	16	12639800	PRDX5	6.43	0.81	0.14	0.44
PRMT2	ILMN-1675098	rs1028231	21	47931653	C21ORF57	rs958127	18	31497346		7.34	0.53	0.11	0.25
PRMT2	ILMN-1675098	rs2382372	21	48063862		rs11701058	21	47776382	C21ORF57	4.81	0.19	0.03	0.04
PSMB1	ILMN-1789176	rs38962607	18	43983954		rs13207114	6	170877444	PSMB1	5.79	0.44	0.21	0.27
PSMB1	ILMN-1789176	rs6060930	20	30347832		rs6928843	6	170890384	PSMB1	5.14	0.44	0.21	0.27
PSMB1	ILMN-1789176	rs6928843	6	170890384	PSMB1	rs9295415	6	170823379	PSMB1	5.44	1.95	0.64	1.78
PSMB1	ILMN-1789176	rs7298749	12	13172816		rs2769689	1	225779957	PSMB1	4.58	1.18	0.32	0.86
PWPI	ILMN-1743049	rs2353567	14	95478823		rs13207114	6	170877444	PSMB1	5.42	1.03	0.48	0.15
PWPI	ILMN-1743049	rs4969205	17	76598123		rs11036212	11	5221825	PSMB1	5.00	0.03	0.48	0.15
PWPI	ILMN-1743049	rs631562	11	126852438		rs11036212	11	5221825	PSMB1	5.90	0.80	0.08	0.38
QDPR	ILMN-1672443	rs4946705	6	106348246		rs10020773	4	17526682	PSMB1	5.70	0.02	0.40	0.11
RAB3IP	ILMN-1803197	rs241730	22	33375704		rs7905307	12	70235726	QDPR	6.55	1.03	1.25	1.55
RABAC1	ILMN-2207363	rs1075728	19	42462788	RABAC1	rs79051628	11	120161117		6.42	0.28	0.84	0.59
RBL2	ILMN-1756999	rs9931702	16	53526551	AKTIP	rs1863464	15	26988488		6.38	0.03	0.31	0.08
RCN1	ILMN-1800276	rs10879131	12	41147155		rs4922579	11	32136436	RCN1	5.23	0.58	0.37	0.43
RCN1	ILMN-1800276	rs4922579	11	32136436	RCN1	rs1166957	8	141177468		4.32	0.41	0.09	0.17
RCN1	ILMN-1800276	rs4922579	11	32136436	RCN1					5.40	0.04	0.26	0.07

Continued on next page

Table S1 – continued from previous page

Gene ID ^a			Expression trait			SNP 1			SNP 2			Interaction statistic ^f			BGS ^g			-log ₁₀ p-values			Distance / Mb ^b		
Gene	ID ^a	Chr.	rs ID	Chr.	Pos/Mb ^c	Association ^d	rs ID	Chr.	Pos/Mb ^c	Association ^d	rs ID	Chr.	Pos/Mb ^c	F _{DR}	F _{DR} max	Meta ^g	EGCUT ^e	Meta ^g	EGCUT ^e	Meta ^g	EGCUT ^e	Distance / Mb ^b	
RENE	ILMN_1802830	1	rs4982958	14	24987865		rs301819	1	8501786	RENE	rs301819	1	8501786	5.66	0.61	1.23	1.17						
RENE	ILMN_1802838	1	rs7697290	4	135248366		rs301819	1	8501786	RENE	rs301819	1	8501786	5.74	0.14	0.10	0.06						
RENE	ILMN_1802840	1	rs11085629	19	13174312		rs301819	1	8501786	RENE	rs301819	1	8501786	5.12	0.21	0.33	0.21						
RENE	ILMN_1802842	1	rs301819	3	12844086		rs301819	1	8501786	RENE	rs301819	1	8501786	5.71	0.08	0.60	0.26						
RENE	ILMN_1802844	1	rs301819	3	12844086	RNASE6	rs301819	1	8501786	RENE	rs301819	1	8501786	5.71	0.08	0.60	0.26						
RENE	ILMN_1802846	1	rs301819	3	12844086	RNASE6	rs301819	1	8501786	RENE	rs301819	1	8501786	5.71	0.08	0.60	0.26						
RENE	ILMN_1802848	1	rs301819	3	12844086	RNASE6	rs301819	1	8501786	RENE	rs301819	1	8501786	5.71	0.08	0.60	0.26						
RENE	ILMN_1802850	1	rs301819	3	12844086	RNASE6	rs301819	1	8501786	RENE	rs301819	1	8501786	5.71	0.08	0.60	0.26						
RENE	ILMN_1802852	1	rs301819	3	12844086	RNASE6	rs301819	1	8501786	RENE	rs301819	1	8501786	5.71	0.08	0.60	0.26						
RENE	ILMN_1802854	1	rs301819	3	12844086	RNASE6	rs301819	1	8501786	RENE	rs301819	1	8501786	5.71	0.08	0.60	0.26						
RENE	ILMN_1802856	1	rs301819	3	12844086	RNASE6	rs301819	1	8501786	RENE	rs301819	1	8501786	5.71	0.08	0.60	0.26						
RENE	ILMN_1802858	1	rs301819	3	12844086	RNASE6	rs301819	1	8501786	RENE	rs301819	1	8501786	5.71	0.08	0.60	0.26						
RENE	ILMN_1802860	1	rs301819	3	12844086	RNASE6	rs301819	1	8501786	RENE	rs301819	1	8501786	5.71	0.08	0.60	0.26						
RENE	ILMN_1802862	1	rs301819	3	12844086	RNASE6	rs301819	1	8501786	RENE	rs301819	1	8501786	5.71	0.08	0.60	0.26						
RENE	ILMN_1802864	1	rs301819	3	12844086	RNASE6	rs301819	1	8501786	RENE	rs301819	1	8501786	5.71	0.08	0.60	0.26						
RENE	ILMN_1802866	1	rs301819	3	12844086	RNASE6	rs301819	1	8501786	RENE	rs301819	1	8501786	5.71	0.08	0.60	0.26						
RENE	ILMN_1802868	1	rs301819	3	12844086	RNASE6	rs301819	1	8501786	RENE	rs301819	1	8501786	5.71	0.08	0.60	0.26						
RENE	ILMN_1802870	1	rs301819	3	12844086	RNASE6	rs301819	1	8501786	RENE	rs301819	1	8501786	5.71	0.08	0.60	0.26						
RENE	ILMN_1802872	1	rs301819	3	12844086	RNASE6	rs301819	1	8501786	RENE	rs301819	1	8501786	5.71	0.08	0.60	0.26						
RENE	ILMN_1802874	1	rs301819	3	12844086	RNASE6	rs301819	1	8501786	RENE	rs301819	1	8501786	5.71	0.08	0.60	0.26						
RENE	ILMN_1802876	1	rs301819	3	12844086	RNASE6	rs301819	1	8501786	RENE	rs301819	1	8501786	5.71	0.08	0.60	0.26						
RENE	ILMN_1802878	1	rs301819	3	12844086	RNASE6	rs301819	1	8501786	RENE	rs301819	1	8501786	5.71	0.08	0.60	0.26						
RENE	ILMN_1802880	1	rs301819	3	12844086	RNASE6	rs301819	1	8501786	RENE	rs301819	1	8501786	5.71	0.08	0.60	0.26						
RENE	ILMN_1802882	1	rs301819	3	12844086	RNASE6	rs301819	1	8501786	RENE	rs301819	1	8501786	5.71	0.08	0.60	0.26						
RENE	ILMN_1802884	1	rs301819	3	12844086	RNASE6	rs301819	1	8501786	RENE	rs301819	1	8501786	5.71	0.08	0.60	0.26						
RENE	ILMN_1802886	1	rs301819	3	12844086	RNASE6	rs301819	1	8501786	RENE	rs301819	1	8501786	5.71	0.08	0.60	0.26						
RENE	ILMN_1802888	1	rs301819	3	12844086	RNASE6	rs301819	1	8501786	RENE	rs301819	1	8501786	5.71	0.08	0.60	0.26						
RENE	ILMN_1802890	1	rs301819	3	12844086	RNASE6	rs301819	1	8501786	RENE	rs301819	1	8501786	5.71	0.08	0.60	0.26						
RENE	ILMN_1802892	1	rs301819	3	12844086	RNASE6	rs301819	1	8501786	RENE	rs301819	1	8501786	5.71	0.08	0.60	0.26						
RENE	ILMN_1802894	1	rs301819	3	12844086	RNASE6	rs301819	1	8501786	RENE	rs301819	1	8501786	5.71	0.08	0.60	0.26						
RENE	ILMN_1802896	1	rs301819	3	12844086	RNASE6	rs301819	1	8501786	RENE	rs301819	1	8501786	5.71	0.08	0.60	0.26						
RENE	ILMN_1802898	1	rs301819	3	12844086	RNASE6	rs301819	1	8501786	RENE	rs301819	1	8501786	5.71	0.08	0.60	0.26						
RENE	ILMN_1802900	1	rs301819	3	12844086	RNASE6	rs301819	1	8501786	RENE	rs301819	1	8501786	5.71	0.08	0.60	0.26						
RENE	ILMN_1802902	1	rs301819	3	12844086	RNASE6	rs301819	1	8501786	RENE	rs301819	1	8501786	5.71	0.08	0.60	0.26						
RENE	ILMN_1802904	1	rs301819	3	12844086	RNASE6	rs301819	1	8501786	RENE	rs301819	1	8501786	5.71	0.08	0.60	0.26						
RENE	ILMN_1802906	1	rs301819	3	12844086	RNASE6	rs301819	1	8501786	RENE	rs301819	1	8501786	5.71	0.08	0.60	0.26						
RENE	ILMN_1802908	1	rs301819	3	12844086	RNASE6	rs301819	1	8501786	RENE	rs301819	1	8501786	5.71	0.08	0.60	0.26						
RENE	ILMN_1802910	1	rs301819	3	12844086	RNASE6	rs301819	1	8501786	RENE	rs301819	1	8501786	5.71	0.08	0.60	0.26						
RENE	ILMN_1802912	1	rs301819	3	12844086	RNASE6	rs301819	1	8501786	RENE	rs301819	1	8501786	5.71	0.08	0.60	0.26						
RENE	ILMN_1802914	1	rs301819	3	12844086	RNASE6	rs301819	1	8501786	RENE	rs301819	1	8501786	5.71	0.08	0.60	0.26						
RENE	ILMN_1802916	1	rs301819	3	12844086	RNASE6	rs301819	1	8501786	RENE	rs301819	1	8501786	5.71	0.08	0.60	0.26						
RENE	ILMN_1802918	1	rs301819	3	12844086	RNASE6	rs301819	1	8501786	RENE	rs301819	1	8501786	5.71	0.08	0.60	0.26						
RENE	ILMN_1802920	1	rs301819	3	12844086	RNASE6	rs301819	1	8501786	RENE	rs301819	1	8501786	5.71	0.08	0.60	0.26						
RENE	ILMN_1802922	1	rs301819	3	12844086	RNASE6	rs301819	1	8501786	RENE	rs301819	1	8501786	5.71	0.08	0.60	0.26						
RENE	ILMN_1802924	1	rs301819	3	12844086	RNASE6	rs301819	1	8501786	RENE	rs301819	1	8501786	5.71	0.08	0.60	0.26						
RENE	ILMN_1802926	1	rs301819	3	12844086	RNASE6	rs301819	1	8501786	RENE	rs301819	1	8501786	5.71	0.08	0.60	0.26						
RENE	ILMN_1802928	1	rs301819	3	12844086	RNASE6	rs301819	1	8501786	RENE	rs301819	1	8501786	5.71	0.08	0.60	0.26						
RENE	ILMN_1802930	1	rs301819	3	12844086	RNASE6	rs301819	1	8501786	RENE	rs301819	1	8501786	5.71	0.08	0.60	0.26						
RENE	ILMN_1802932	1	rs301819	3	12844086	RNASE6	rs301819	1	8501786	RENE	rs301819	1	8501786	5.71	0.08	0.60	0.26						
RENE	ILMN_1802934	1	rs301819	3	12844086	RNASE6	rs301819	1	8501786	RENE	rs301819	1	8501786	5.71	0.08	0.60	0.26						
RENE	ILMN_1802936	1	rs301819	3	12844086	RNASE6	rs301819	1	8501786	RENE	rs301819	1	8501786	5.71	0.08	0.60	0.26						
RENE	ILMN_1802938	1	rs301819	3	12844086	RNASE6	rs301819	1	8501786	RENE	rs301819	1	8501786	5.71	0.08	0.60	0.26						
RENE	ILMN_1802940	1	rs301819	3	12844086	RNASE6	rs301819	1	8501786	RENE	rs301819	1	8501786	5.71	0.08	0.60	0.26						
RENE	ILMN_1802942	1	rs301819	3	12844086	RNASE6	rs301819	1	8501786	RENE	rs301819	1	8501786	5.71	0.08	0.60	0.26						
RENE	ILMN_1802944	1	rs301819	3	12844086	RNASE6	rs301819	1	8501786	RENE	rs301819	1	8501786	5.71	0.08	0.60	0.26						
RENE	ILMN_1802946	1	rs301819	3	12844086	RNASE6	rs301819	1	8501786	RENE	rs301819	1	8501786	5.71	0.08	0.60	0.26						
RENE	ILMN_1802948	1	rs301819	3	12844086	RNASE6	rs301819	1	8501786	RENE	rs301819	1	8501786	5.71	0.08	0.60	0.26						
RENE	ILMN_1802950	1	rs301819	3	12844086	RNASE6	rs301819	1	8501786	RENE	rs301819	1	8501786	5.71	0.08	0.60	0.26						
RENE	ILMN_1802952	1	rs301819	3	12844086	RNASE6	rs301819	1	8501786	RENE	rs301819	1	8501786	5.71	0.08	0.60	0.26						
RENE	ILMN_1802954	1	rs301819	3	12844086	RNASE6	rs301819	1	8501786	RENE	rs301819	1	8501786	5.71	0.08	0.60	0.26						
RENE	ILMN_1802956	1	rs301819	3	12844086	RNASE6	rs301819	1	8501786	RENE	rs301819	1	8501786	5.71	0.08	0.60	0.26						
RENE	ILMN_1802958	1	rs301819	3	12844086	RNASE6	rs301819	1	8501786	RENE	rs301819	1	8501786	5.71	0.08	0.60	0.26						
RE																							

Continued on next page

Table S1 – continued from previous page

Gene ID ^a	Expression trait		SNP 1			SNP 2			Interaction statistic / -log ₁₀ p-values						
	Probe ID ^b	Chr.	rs ID	Chr.	Pos/Mb ^c	Association ^d	rs ID	Chr.	Pos/Mb ^c	Association ^d	BSGS ^e	Fehrmann ^f	EGCUT ^g	Meta ^g	Distance / Mb ^h
TMED4	ILMN-1804148	7	rs1940400	11	132389627		rs17725246	7	44581986	TMED4	3.70	0.06	1.34	0.70	
TMEM149	ILMN-1786426	19	rs28390126	21	47248981		rs8106959	19	36219525	TMEM149	8.11	0.16	0.48	0.26	
TMEM149	ILMN-1786426	19	rs75762335	22	27923288		rs8106959	19	36219525	TMEM149	6.79				
TMEM149	ILMN-1786426	19	rs6090518	20	43207005		rs8106959	19	36219525	TMEM149	11.09	0.76			
TMEM149	ILMN-1786426	19	rs807491	19	36268923	SNX26	rs72546001	19	36147315	TMEM149	12.16	81.55	45.78	145.78	0.122
TMEM149	ILMN-1786426	19	rs8106959	19	36219525	TMEM149	rs10916259	9	133025756		8.02	1.55	3.09	3.07	
TMEM149	ILMN-1786426	19	rs8106959	19	36219525	TMEM149	rs10937361	3	188395436		8.39	0.40	0.99	0.80	
TMEM149	ILMN-1786426	19	rs8106959	19	36219525	TMEM149	rs1401098	12	128884559		7.37	2.41	1.00	2.52	
TMEM149	ILMN-1786426	19	rs8106959	19	36219525	TMEM149	rs15572935	18	64268976		6.95	0.08	0.07	0.03	
TMEM149	ILMN-1786426	19	rs8106959	19	36219525	TMEM149	rs17719594	14	90932398		6.93	3.06	0.77	2.87	
TMEM149	ILMN-1786426	19	rs8106959	19	36219525	TMEM149	rs1843357	8	13822381		6.21	3.72	3.33	6.00	
TMEM149	ILMN-1786426	19	rs8106959	19	36219525	TMEM149	rs2531458	4	113317583		7.30	0.04	9.61	8.00	
TMEM149	ILMN-1786426	19	rs8106959	19	36219525	TMEM149	rs2539000	7	147619772		6.70	1.57	1.52	2.27	
TMEM149	ILMN-1786426	19	rs8106959	19	36219525	TMEM149	rs2731711	5	171792273		5.92	0.19	0.33	0.19	
TMEM149	ILMN-1786426	19	rs8106959	19	36219525	TMEM149	rs4711728	11	129595460		8.90	0.90	3.62	3.51	
TMEM149	ILMN-1786426	19	rs8106959	19	36219525	TMEM149	rs6718480	2	233879066		8.55	3.31	5.15	7.36	
TMEM149	ILMN-1786426	19	rs8106959	19	36219525	TMEM149	rs6926382	2	161683974		5.80	3.06	8.80	10.72	
TMEM149	ILMN-1786426	19	rs8106959	19	36219525	TMEM149	rs7213338	17	80357420		5.49	0.07	3.14	2.10	
TMEM149	ILMN-1786426	19	rs8106959	19	36219525	TMEM149	rs914940	1	242889492		6.22	3.36	6.96	9.20	
TMEM149	ILMN-1786426	19	rs8106959	19	36219525	TMEM149	rs9509428	13	21473932		9.44	0.10	5.75	4.47	
TMEM63A	ILMN-1796439	1	rs1254086	13	72890603		rs4149226	1	226027323	TMEM63A	5.60	0.64	0.12	0.32	
TMEM80	ILMN-1768482	11	rs1548475	9	58058246		rs4963126	11	656845	TMEM80	5.79	0.11	0.15	0.07	
TNP03	ILMN-1683811	7	rs1537146	9	4859303		rs10488630	7	128593948	IRF5	5.51	1.03	0.17	0.62	
TNP03	ILMN-1683811	7	rs199793	20	22827303		rs10488630	7	128593948	IRF5	5.52	3.19	1.89	4.09	
TRA2A	ILMN-1731043	7	rs1776572	13	113531675		rs1770192	7	23493358		8.23	0.28	0.40	0.29	0.031
TRAPPC4	ILMN-1814650	11	rs1793823	11	7751894		rs3916581	11	11888787	TRAPPC4	5.51	0.93	0.01	0.36	
TRAPPC5	ILMN-2372639	19	rs17159840	19	7758194	TRAPPC5	rs10059004	4	166970604	TRAPPC4	5.52	0.37	1.60	1.07	12.131
TRAPPC5	ILMN-2372639	19	rs17159840	19	7758194	TRAPPC5	rs1023095	8	132022957		6.92	0.21	0.68	0.68	
TRAPPC5	ILMN-2372639	19	rs17159840	19	7758194	TRAPPC5	rs1375714	6	156404902		7.79	0.12	0.18	0.08	
TRAPPC5	ILMN-2372639	19	rs17159840	19	7758194	TRAPPC5	rs1393299	1	242329701		6.43	0.63	0.47	0.59	
TRAPPC5	ILMN-2372639	19	rs17159840	19	7758194	TRAPPC5	rs17763599	19	2369415		6.38	0.21	0.24	0.16	
TRAPPC5	ILMN-2372639	19	rs17159840	19	7758194	TRAPPC5	rs4068328	17	57495435		6.51	0.50	0.34	0.44	
TRAPPC5	ILMN-2372639	19	rs17159840	19	7758194	TRAPPC5	rs7313362	12	129644342		7.08	0.04	0.65	0.25	
TRAPPC5	ILMN-2372639	19	rs17159840	19	7758194	TRAPPC5	rs7694997	4	9947811		5.86	0.20	0.36	0.22	
TRAPPC5	ILMN-2372639	19	rs17159840	19	7758194	TRAPPC5	rs800935	7	146690926		6.27	0.15	0.33	0.16	
TRAPPC5	ILMN-2372639	19	rs17159840	19	7758194	TRAPPC5	rs856638	14	85439550		6.73	0.24	0.07	0.08	
TRAPPC5	ILMN-2372639	19	rs380708	22	22740855		rs17159840	19	7758194	TRAPPC5	7.58	0.85	0.78	1.01	
TRAPPC5	ILMN-2372639	19	rs3916995	19	45128454		rs17159840	19	7758194	TRAPPC5	7.73	0.51	0.55	0.56	
TRAPPC5	ILMN-2372639	19	rs6040514	20	11272861		rs10179572	2	228504503	TRAPPC5	8.10	0.14	0.02	0.02	
TRAPPC5	ILMN-2372639	19	rs7246264	19	7762978		rs10179572	2	228504503	TRAPPC5	6.71	0.14	0.26	0.13	
TRAPPC5	ILMN-2372639	19	rs7246264	19	7762978		rs12921440	16	30408705		7.34	0.08	0.86	0.40	
TRAPPC5	ILMN-2372639	19	rs7246264	19	7762978		rs1887778	3	157393770	RAPGEF1	7.05	0.08	0.86	0.40	
TRAPPC5	ILMN-2372639	19	rs7246264	19	7762978		rs963354	3	157393770	RAPGEF1	7.41	0.36	0.90	0.69	
TREM1	ILMN-1688231	6	rs10862975	12	85749398		rs2395771	6	41264577	TREM1	5.42	0.11	0.25	0.11	
TREM1	ILMN-1688231	6	rs2527180	17	158808416		rs2395771	6	41264577	TREM1	5.92	1.20	1.23	1.69	
TRIM38	ILMN-1697971	6	rs2527180	17	158808416		rs2032447	6	26044369	TRIM38	6.46	0.04	0.91	0.39	
TSPAN14	ILMN-1785060	10	rs968726	7	27194634	MYBPC3	rs10748526	10	82273079	TSPAN14	6.00	0.07	0.18	0.06	
TSPAN32	ILMN-178621	11	rs10838738	11	47663049	MYBPC3	rs12800098	11	2317951	TSPAN32	5.01				45.345
TSPAN32	ILMN-2389070	11	rs12800098	11	2317951	TSPAN32	rs620607	6	137947208	TSPAN32	5.51				
TYP	ILMN-323126	22	rs140522	22	50971266	ECGF1	rs1198819	2	238746880	TYP	6.34				
TYP	ILMN-323126	22	rs470119	22	50966914	ECGF1	rs4783126	16	85147633	TYP	6.13				

Continued on next page

Table S1 – continued from previous page

Expression trait			SNP 1			SNP 2			Interaction statistic ^f / $-\log_{10}$ p -values			Distance / Mb ^h		
Gene ID ^a	Probe ID ^b	Chr.	rs ID	Chr.	Pos / Mb ^c	Association ^d	rs ID	Chr.	SNP-2	Association ^d	BSGS ^e	Fehrmann ^f	EGCUT ^g	Meta ^g
UBASH3A	LMN-2338348	21	rs1893592	21	43855067	UBASH3A	rs7201194	16	83600397		5.91	0.59	0.42	0.52
UBASH3A	LMN-2338348	21	rs1893592	21	43855067	UBASH3A	rs7201194	16	83600397		6.01	0.48	1.29	1.10
USP36	LMN-1697227	17	rs2279308	17	76794981	USP36	rs7225546	17	75151717		5.71	0.03	0.14	0.03
VASP	LMN-1743646	19	rs1264226	19	40063167		rs2276470	19	45974668		5.09	0.94	5.14	4.95
VNN2	LMN-1678939	6	rs10435352	7	103252718		rs1883613	6	133077063	VNN2	5.64	0.84	0.15	0.46
VNN2	LMN-1678939	6	rs10435352	7	103252718		rs1883613	6	133077063	VNN2	5.64	0.84	0.15	0.46
VNN2	LMN-1678939	6	rs134447	20	49927332		rs1883617	6	133072650	VNN2	5.44	0.39	0.69	0.57
VNN2	LMN-1678939	6	rs134447	20	49927332		rs1883617	6	133072650	VNN2	5.44	0.39	0.69	0.57
VNN3	LMN-1678939	6	rs216495	11	16834510		rs1883617	6	133072650	VNN2	5.77	0.33	0.19	0.19
VNN3	LMN-1678939	6	rs10278073	7	151662184		rs2267952	6	133067782	VNN3	6.44	0.16	0.74	0.41
VNN3	LMN-1804935	6	rs1443946	8	73006453		rs2267952	6	133067782	VNN3	5.74	0.23	0.48	0.31
VNN3	LMN-1804935	6	rs348462	9	75547169		rs2267952	6	133067782	VNN3	6.44	0.31	0.17	0.17
VNN3	LMN-1804935	6	rs7157055	14	83262064		rs2267952	6	133067782	VNN3	5.82	0.03	0.19	0.04
VNN3	LMN-2387680	6	rs2823165	21	5694253		rs2267952	6	133067782	VNN3	6.12	0.73	1.15	1.21
VNN3	LMN-2387680	6	rs9596457	13	51692548		rs2267952	6	133067782	VNN3	4.83	0.46	0.05	0.16
VSTM1	LMN-1763455	19	rs9596457	19	54553697	VSTM1	rs4532100	18	71024750		5.60	0.53	0.54	0.57
VSTM1	LMN-1763455	19	rs10500316	19	54553697	VSTM1	rs7895870	10	123098249		5.71	0.48	0.17	0.26
VSTM1	LMN-1763455	19	rs10500316	19	54553697	VSTM1	rs7895870	10	123098249		5.71	0.48	0.17	0.26
VSTM1	LMN-1763455	19	rs9628570	22	30261219		rs10500316	19	54553697	VSTM1	5.88	0.81	1.38	1.47
WDR48	LMN-1762103	3	rs1889783	3	188927822		rs10500316	19	54553697	VSTM1	5.88	0.81	1.38	1.47
WDR48	LMN-1762103	3	rs1889783	3	188927822		rs6778963	3	39091812	WDR48	5.88	0.19	0.13	0.09
WDR48	LMN-1762103	3	rs1887778	9	134635088		rs883349	3	39067925	WDR48	6.34	0.57	1.35	1.22
WDR6	LMN-1669484	3	rs9554833	13	102624790		rs7619193	3	39044131	WDR48	5.85	0.18	0.61	0.35
WDR6	LMN-1669484	3	rs12362253	11	123371708		rs7619193	3	39044131	WDR48	5.85	0.18	0.61	0.35
XAF1	LMN-2330573	17	rs1533031	17	9673170	XAF1	rs11715581	3	49194331	WDR6	4.86	1.64	1.43	2.25
XAF1	LMN-2330573	17	rs1533031	17	9673170	XAF1	rs12591171	15	68179799		5.48	2.38	0.17	1.63
ZFP90	LMN-1684628	16	rs909446	21	37040648		rs1812968	16	93573945	ZFP90	5.79	0.09	0.36	0.10
ZNF500	LMN-1700238	16	rs4283723	22	48283177		rs2290560	16	4799041	ZNF500	5.29	0.67	0.27	0.46
ZNF500	LMN-1700238	16	rs4283723	22	48283177		rs2290560	16	4799041	ZNF500	5.29	0.67	0.27	0.46
ZYX	LMN-1701875	7	rs6056281	20	8935312		rs2242601	7	143093824	ZYX	6.04	0.26	0.01	0.05

^a Phenotypes are expression levels of RefSeq Genes^b Illumina probe ID used to measure gene expression^c Physical SNP position in base pairs (HG19)^d RefSeq Gene ID of gene expression level that is influenced by the SNP (BSGS discovery dataset, significance threshold = 1.29 × 10⁻¹¹)^e Interaction – log₁₀ p -value from discovery dataset^f Interaction – log₁₀ p -value from replication dataset^g Interaction – log₁₀ p -value from meta analysis of replication datasets only^h Distance in Mb between interacting SNPs for *cis-cis* acting SNP pairsⁱ p -values are absent if the interaction did not pass the QC filtering in the replication dataset^j Meta analysis p -values are absent if the interaction did not pass the QC filtering in either replication dataset

Table S2: **Estimation of additive and non-additive variance components from pedigree information** Taken from previous analysis in Powell et al 2013²²

Gene	Probe	Additive		Non-additive	
		Variance	s.e.	Variance	s.e.
NAPRT1	ILMN_1710752	0.37	0.03	0.14	0.05
TMEM149	ILMN_1786426	0.41	0.04	0.09	0.04
MBNL1	ILMN_2313158	0.18	0.03	0.11	0.04
TRAPPC5	ILMN_2372639	0.32	0.04	0.13	0.05
CAST	ILMN_1717234	0.31	0.03	0.10	0.04

Table S3: **Concordance of sign of epistatic variance components between discovery and replication datasets**

Test	Interactions ^a	Dataset	n^b	Expected ^c	Observed ^d	p -value
1 ^e	All	EGCUT	434	217.00	306	6.69×10^{-18}
		Fehrmann	434	217.00	278	5.04×10^{-9}
		Both	434	108.50	221	5.56×10^{-31}
	Significant	EGCUT	30	15.00	25	3.25×10^{-4}
		Fehrmann	30	15.00	24	1.43×10^{-3}
		Both	30	7.50	22	3.76×10^{-8}
2 ^f	All	EGCUT	434	54.25	92	4.22×10^{-7}
		Fehrmann	434	54.25	79	6.18×10^{-4}
		Both	434	6.78	30	2.55×10^{-11}
	Significant	EGCUT	30	3.75	19	9.46×10^{-11}
		Fehrmann	30	3.75	19	9.46×10^{-11}
		Both	30	0.47	18	2.23×10^{-25}
3 ^g	All	EGCUT	1133	566.50	775	7.10×10^{-36}
		Fehrmann	1133	566.50	726	1.90×10^{-21}
		Both	1133	283.25	562	1.39×10^{-70}
	Significant	EGCUT	73	36.50	55	1.69×10^{-5}
		Fehrmann	73	36.50	55	1.69×10^{-5}
		Both	73	18.25	46	7.86×10^{-12}

^a “All” denotes 434 discovery interactions and “Significant” denotes 30 interactions with significant replication p -values

^b Number of tests for concordance

^c Expected number of concordant cases under the null hypothesis of no interactions

^d Observed number of concordant cases

^e The sign of the most significant epistatic variance component in discovery is the same as the corresponding variance component in the replication data.

^f The largest epistatic variance component in the discovery is the same as in the replication with the same sign in both.

^g The sign of all epistatic variance components in the discovery with $p < 0.05$ are the same as the corresponding variance components in the replication data.

Table S4: **Concordance of sign of epistatic variance components between discovery and replication datasets using test 4**

Interactions ^a	Dataset	n^b	0 ^c	1 ^c	2 ^c	3 ^c	4 ^c	p
Expected ^d	-	-	0.06	0.25	0.38	0.25	0.06	-
All	EGCUT	434	0.06	0.22	0.41	0.23	0.08	0.194
All	Fehrman	434	0.07	0.22	0.39	0.24	0.08	0.385
All	Combined	868	0.07	0.22	0.40	0.23	0.08	0.0448
Significant	EGCUT	30	0.07	0.03	0.30	0.33	0.27	4.72×10^{-4}
Significant	Fehrman	30	0.03	0.07	0.33	0.27	0.30	6.69×10^{-4}
Significant	Combined	60	0.05	0.05	0.32	0.30	0.28	5.49×10^{-8}

^a “All” denotes 434 discovery interactions and “Significant” denotes 30 interactions with significant replication p -values.

^b Number of tests for concordance.

^c Proportion of tests that have 0, 1, 2, 3 or 4 concordant signs between discovery and replication.

^d Expected proportion of concordant signs under the null hypothesis of no epistasis.

Table S5: Details on linkage disequilibrium and relative positions of all discovery interactions with SNPs on the same chromosome

Chr	Gene	SNP 1	SNP 2	Position 1	Position 2	Distance / Mb	R^2	D'
19	TMEM149	rs807491	rs7254601	36268923	36147315	0.122	0.000	0.001
17	FN3KRP	rs898095	rs9892064	80890638	80827903	0.063	0.063	0.088
21	CSTB	rs9979356	rs3761385	45230974	45198355	0.033	0.041	0.066
3	MBNL1	rs16864367	rs13079208	152234166	152116652	0.118	0.041	0.117
10	ADK	rs2395095	rs10824092	76446305	75929517	0.517	0.013	0.020
11	CTSC	rs7930237	rs556895	88117962	88077479	0.040	0.012	0.045
17	GAA	rs11150847	rs12602462	78153130	78146016	0.007	0.000	0.001
8	NAPRT1	rs2123758	rs3889129	144663661	144613680	0.050	0.053	0.060
1	LAX1	rs1891432	rs10900520	203877662	203780591	0.097	0.065	0.106
18	MBP	rs8092433	rs4890876	74747424	74732087	0.015	0.035	0.053
11	SNORD14A	rs2634462	rs6486334	17339127	17015557	0.324	0.008	0.012
21	C21ORF57	rs9978658	rs11701361	48027084	47764477	0.263	0.032	0.065
16	RPL13	rs352935	rs2965817	89648580	89513234	0.135	0.054	0.060
19	ATP13A1	rs4284750	rs873870	19810050	19738554	0.071	0.008	0.015
2	NCL	rs7563453	rs4973397	232301670	232291471	0.010	0.027	0.029
5	HNRPH1	rs6894268	rs4700810	179032488	178991794	0.041	0.000	0.001
19	VASP	rs1264226	rs2276470	46063167	45974668	0.088	0.018	0.022
7	TRA2A	rs7776572	rs11770192	23528927	23498358	0.031	0.064	0.064
21	PRMT2	rs2839372	rs11701058	48063862	47776382	0.287	0.100	0.122
12	OAS1	rs13311	rs2072133	113448652	113409260	0.039	0.002	0.016
16	N4BP1	rs12444224	rs11649236	87580855	48632478	38.948	0.007	0.021
5	CAST	rs12719343	rs7733671	125369113	96000269	29.369	0.001	0.001
7	DNAJB6	rs2286842	rs3779589	157216093	157163614	0.052	0.005	0.006
1	OVGP1	rs10802822	rs1264898	240132968	111992823	128.140	0.008	0.030
20	CD93	rs2868504	rs1884655	37771578	23074375	14.697	0.000	0.002
11	PHCA	rs493642	rs10736812	123097386	76708086	46.389	0.002	0.008
21	MX1	rs459498	rs8130120	42795027	29363604	13.431	0.000	0.000
16	AKTIP	rs2896940	rs13332406	57721127	53489705	4.231	0.000	0.001
17	CDK5R1	rs9905940	rs11655031	46614102	30833162	15.781	0.000	0.000
2	CYBRD1	rs888427	rs7591849	172368120	160112881	12.255	0.000	0.000
8	HMBOX1	rs587639	rs7837237	132725731	28876221	103.850	0.001	0.001
11	TRAPPC4	rs1793823	rs3916581	131018917	118887887	12.131	0.001	0.002
12	PEX5	rs10444467	rs4329748	128052636	7364442	120.688	0.000	0.000
12	FLJ20489	rs17615703	rs3782908	117036766	48169526	68.867	0.001	0.002
16	PRKCB1	rs2188355	rs10492793	23867776	12639800	11.228	0.000	0.000
14	MRPL52	rs1950857	rs3811188	26710271	23299135	3.411	0.002	0.004
17	C17ORF60	rs9907897	rs7405659	63502633	59874129	3.629	0.004	0.011
6	FLJ43093	rs6906101	rs13214069	36667610	32705248	3.962	0.000	0.000
19	TRAPPC5	rs17159840	rs17763599	7758194	2369415	5.389	0.000	0.000
22	PISD	rs715572	rs6518754	33234931	32097775	1.137	0.001	0.003
12	DIP2B	rs871257	rs12427378	117994348	51074199	66.920	0.001	0.001
12	GPR162	rs2272500	rs2707210	79685913	6902002	72.784	0.003	0.005
17	USP36	rs2279308	rs7225546	76794981	75151717	1.643	0.000	0.000